Politecnico di Torino

Master of Science in Mechanical Engineering

Master's Degree Thesis

Optimization of Heat Release Shapes and Their Impact on Engine Performance

Supervisor

Daniela Anna Misul

Bengt Håkan Johansson

Hadeel Solaka Aronsson

Candidate

Alessandro Bertino

A.A. 2024/2025

Contents

Nomenclature

$\dot{m}_c$	Mass Flow Rate in the Compressor
$\dot{m}_f$	Mass Flow Rate of Fuel
$\dot{m}_t$	Mass Flow Rate in the Turbine
η_b	Brake Efficiency
η_n	Mechanical Efficiency
λ	Air-Fuel Equivalence Ratio
ρ	Fuel Density
C_d	Flow Coefficient
H_u	Lower Heating Value
n_h	Number of Nozzle Holes
NO_x	Nitrogen Oxides
p_1	Compressor Inlet Pressure
p_2	Compressor Outlet Pressure
p_5	Turbine Inlet Pressure
p_6	Turbine Outlet Pressure
P_{comp}	Compressor Pressure
P_{inj}	Injection Pressure
P_{max}	Maximum Pressure in Cylinder
P_c	Compressor Power
P_t	Turbine Power
T_1	Compressor Inlet Temperature
T_5	Turbine Inlet Temperature
V_c	Clearance Volume
V_d	Displacement Volume
W_i	Indicated Work
$X_{\text{O2,air}}$	Theoretical Oxygen Mole Fraction in Fresh Air
X_{O2}	Oxygen Mole Concentration
A	Flow Area
B	Bore
BDC	Bottom Dead Center
BMEP	Brake Mean Effective Pressure

BP	Brake Power
CAD	Crank Angle Degree
CI	Compression Ignition
CO	Carbon Monoxide
CR	Compression Ratio
d	Nozzle Hole Diameter
EGR	Exhaust Gas Recirculation
EVC	Exhaust Valve Closing
HRR	Heat Release Rate
IMEP	Indicated Mean Effective Pressure
IP	Indicated Power
N	Rotational Speed
PM	Particulate Matter
s	Stroke
SFOC	Specific Fuel Oil Consumption
SI	Spark Ignition
SOI	Start of Injection
TDC	Top Dead Center
x	Number of Strokes / 2

Abstract

This study analyzes the heat release rate (HRR) shape and the performance of the G95 marine engine (NOx and Specific Fuel Oil Consumption SFOC), developed by MAN Energy Solutions. The tools used for the analysis are the simulation software GT-Power and MATLAB for post-processing the results.

The engine was studied in both diesel and dual fuel mode (methane main injection with a diesel pilot). For each case, the analysis was done in two conditions: - with "control on" (where parameters like maximum cylinder pressure, compression pressure, Indicated Mean Effective Pressure IMEP, and maximum injection pressure are kept fixed), and with "control off", where fewer limits are applied.

Several engine parameters were changed in order to see the effects on HRR shape and engine performance. These include the fuel nozzle diameter, number of holes, EGR level, and the geometric compression ratio. For the dual fuel mode, pilot injection parameters such as Start Of Injection (SOI), duration, and pilot fuel mass were also varied.

The results show that both engines are already well optimized. In fact, when all the controllers are active, it's hard to get better SFOC values. However, with fewer constraints, better improvements can be reached.

For the diesel engine: - With all controls on, reducing the EGR level from 18.7% to 11.5% results in a slight improvement in SFOC, with a reduction of 0.27%. However, this also causes a significant increase in NO_x emissions, by about 24.45%. Increasing the Geometric compression ratio form 29 to 31 lead to a reduction in NOx of 5.01% without affecting the SFOC

When the control constraints are relaxed (control off), increasing the maximum cylinder pressure from 199 bar to 219 bar leads to a more noticeable SFOC reduction of 1.37%, while the corresponding NO_x increase is 8.92%.

For the dual fuel engine: - With all controls on, lowering the EGR level from 17.8% to 10.5% allows for a 0.51% reduction in SFOC, though NO_x emissions rise by 18.46%. Similarly, increasing the geometric compression ratio from 29 to 33 results in a 0.39% decrease in SFOC, with a NO_x increase of 9.69%. Removing the diesel pilot lead to a reduction of both SFOC and NOx respectively of 0.33% and 7.65%

When the constraints are removed, increasing the maximum cylinder pressure from 198.5 bar to 218.5 bar gives the best SFOC improvement of 1.62%, accompanied by a 16.88% rise in NO_x.

1 Introduction

In recent years, the European Union has worked hard to fight global warming. A big step was taken in 2021 with the European Climate Law [1]. The European Climate Law writes into law the goal set out in the European Green Deal for Europe's economy and society to become climate-neutral by 2050. The law also sets the intermediate target of reducing net greenhouse gas emissions by at least 55% by 2030, compared to 1990 levels.

Climate neutrality by 2050 means achieving net zero greenhouse gas emissions for EU countries as a whole, mainly by cutting emissions, investing in green technologies and protecting the natural environment.

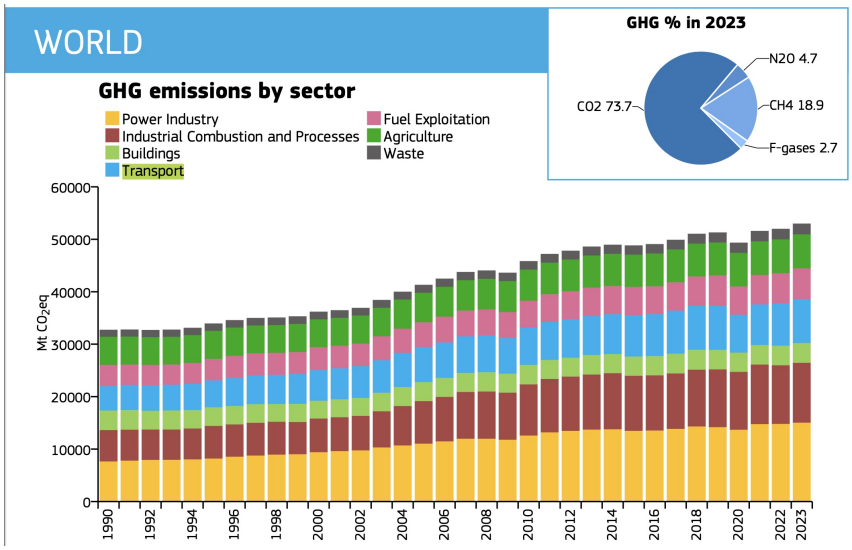

Figure 1: Global Warming sectors distribution [2].

As shown in Figure 1, the transportation sector (blue bars) has a significant impact on global greenhouse gas (GHG) emissions, accounting for around 13%. For this reason, reducing emissions in the transportation sector is a key priority.

Despite advancements in electrification, internal combustion engines (ICEs) continue to play a crucial role in energy production and transportation. This is mainly because renewable energy sources are not always available or easy to store. Additionally, ICEs are particularly advantageous in heavy-duty applications like aviation and maritime transport, where they power aircraft and ships. While electric vehicles have gained popularity in the light-duty sector, electric propulsion faces several challenges, including long charging times, limited battery autonomy, and the lower energy density of batteries. In sectors like aviation, where weight and space constraints are critical, or in the maritime industry, where extremely high energy storage demands are required, electric solutions appear impractical. Consequently, further research and development in internal combustion engine technology remain essential.

Ongoing research in this field focuses on advanced combustion methods, such as Homogeneous Charge Compression Ignition (HCCI), Partially Premixed Combustion (PPC), and Reactivity Controlled Compression Ignition (RCCI), which aim to control combustion processes to increase efficiency and reduce pollution. Additionally, there is growing interest in alternative fuels like methanol, hydrogen, and ammonia, which have low or zero carbon content. These fuels offer the potential to significantly reduce (CO and) CO_2 emissions, and can also be produced in a sustainable, environmentally friendly way.

However, conventional spark ignition (SI) and compression ignition (CI) engines remain the foundation of modern internal combustion technology. SI engines, which operate on homogeneous fuel-air mixtures, generally produce low soot emissions but are limited by knocking and thermal efficiency constraints. On the other hand, CI engines, which operate with diesel fuel,

offer high thermal efficiency but suffer from high soot and NOx emissions due to their heterogeneous fuel-air mixture and high combustion temperatures.

Despite ongoing research into alternative carbon-free fuels, diesel and gasoline are still widely used due to their high availability and the high number of existing engines designed for these fuels.

1.1 Scope of Work

This study investigates the impact of varying engine parameters on heat release rate, fuel consumption, and NOx emissions in a large two-stroke marine engine. The analysis focuses on the G95 engine (G95ME-C10.5-GI-EcoEGR) model developed by MAN Energy Solutions, utilizing the simulation software GT-Power [3].

Due to the presence of numerous controllers that interact with the engine, creating multiple constraints, it is not straightforward to predict the effects of changing a single parameter. Therefore, this study will evaluate the engine's behavior under various constraints, while also exploring potential areas for improvement.

The initial phase of the study examines the engine's performance using diesel as the primary fuel. Subsequently, the investigation extends to methane operation, with diesel used as a pilot fuel.

1.2 Engine Operating Conditions

In this study, the engine operates at 75% of its rated load. The engine is subject to several constraints, which include:

- Maximum cylinder pressure
- Maximum Motoring pressure
- Mantained Maximum injection pressure
- Fixed IMEP (Indicated Mean Effective Pressure)

These constraints vary slightly between the two operating conditions: diesel and methane with a diesel pilot. The values for these constraints under each operating condition are presented in the tables below.

Table 1: Diesel Operating Conditions

P Max [bar]	**P Comp [bar]**	**IMEP [bar]**
199	163	14.04

Table 2: Dual Fuel Operating Conditions

P Max [bar]	**P Comp [bar]**	**IMEP [bar]**
198.5	167.4	14.04

1.3 Engine Description

The engine is a two-stroke model featuring nine cylinders. Each cylinder has a bore of 0.95 m and a stroke of 3.46 m. Each cylinder is equipped with a scavenging port for air intake and an exhaust valve located at the top. The geometric compression ratio of the engine can be adjusted

through the use of shims. Under standard conditions, the geometric compression ratio is 29.5, with the shim thickness being 31 mm.

The engine is equipped with three injectors for diesel fuel and three injectors for methane. It is turbocharged and includes the capability to perform Exhaust Gas Recirculation (EGR) via a blower.

Table 3: Nozzle feature - Diesel Operating Condition

Fuel	**Number of Holes [-] (per injector)**	**Hole Diameter [mm]**
`Diesel`	5	1.7

Table 4: Nozzle feature - Methane Operating Condition

Fuel	**Number of Holes [-]**	**Hole Diameter [mm]**
`Diesel`	3	0.5
`Methane`	5	3.5

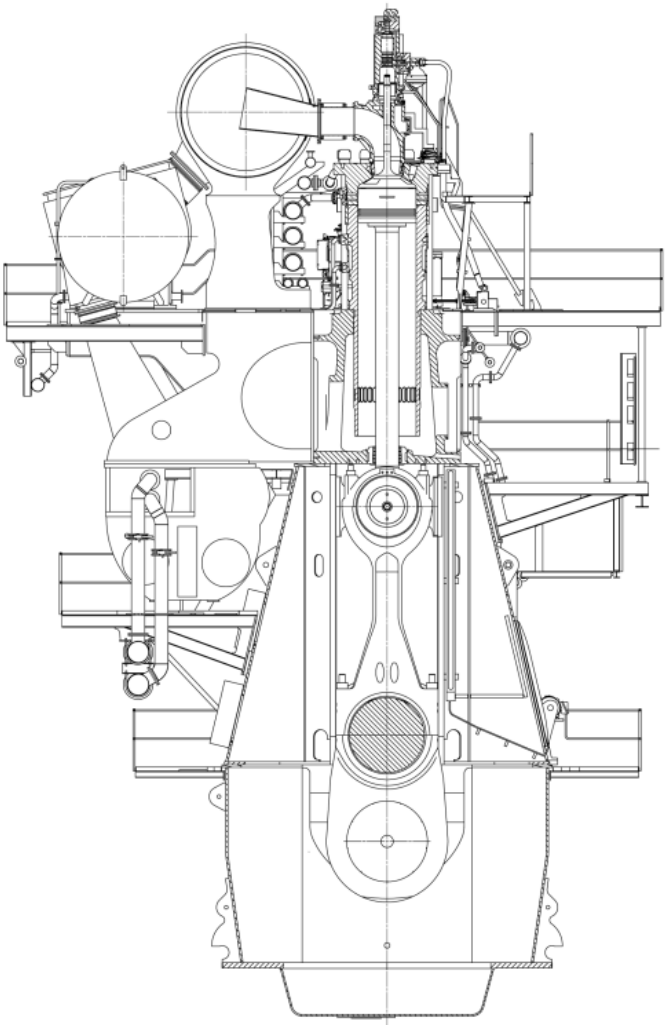

Figure 2: g95 cross section [4].

2 Theoretical background

2.1 Engine parameters

The internal combustion engine allows to convert the fuel energy into mechanical power.
The main components of an engine are:

- Piston,
- Combustion chamber,
- Connecting rod,
- Intake ports and exhaust valve,
- Cranktrain.

Among the geometric parameters of the engine, the most important are:
Displacement volume V_d, defined as:

$$V_d = \frac{\pi}{4} \cdot B^2 \cdot s \tag{1}$$

where:

- B is the bore (cylinder diameter),
- s is the stroke (piston travel length).
- Clearance volume V_c, which is the volume remaining in the cylinder when the piston is at top dead center (TDC).
- Geometric compression ratio CR, defined as the ratio between the total cylinder volume at bottom dead center (BDC) and the clearance volume:

$$CR = \frac{V_d + V_c}{V_c} \tag{2}$$

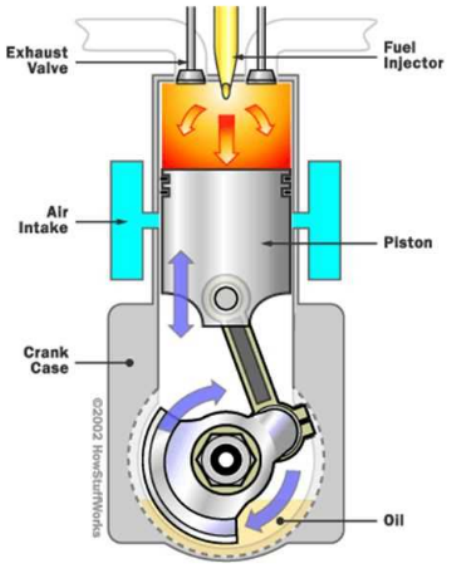

Figure 3: Cylinder geoemtry.

A full engine cycle includes the scavenging, compression, combustion,expansion, and exhaust phases. Among these, it's the expansion phase that actually produces the useful power.

From the indicated work W_i, the Indicated Mean Effective Pressure (IMEP) can be calculated. IMEP is a normalized pressure value that represents the work per unit of engine displacement volume, so it is a good way to compare engines of different size:

$$IMEP = \frac{W_i}{V_d} \tag{3}$$

where V_d is the displacement volume of the engine.

Using IMEP, the indicated power (IP) is given by:

$$IP = \frac{IMEP \cdot V_d \cdot N}{60 \cdot x} \tag{4}$$

where:

- N is the engine rotational speed (RPM),
- x is 2 for 4-stroke engines and 1 for 2-stroke engines.

The brake power (BP) represents the actual useful power delivered at the crankshaft. It can be calculated by multiplying the indicated power (IP) by the mechanical efficiency η_m:

$$BP = \eta_m \cdot IP \tag{5}$$

From a thermodynamic point of view, the engine's brake thermal efficiency η_b is defined as the ratio between the brake power and the fuel energy input:

$$\eta_b = \frac{BP}{\dot{m}_f \cdot H_u} \tag{6}$$

where:

- $\dot{m}_f$ is the fuel mass flow rate,
- H_u is the lower heating value (LHV) of the fuel.

Another common way to express engine performance is through the Specific Fuel Oil Consumption (SFOC), defined as:

$$SFOC = \frac{\dot{m}_f}{BP} \tag{7}$$

which represents the amount of fuel required to produce one unit of brake power.

2.2 2 strokes engine

A two-stroke engine is used to get higher specific power output. Differently from a four-stroke engine, which produces work each two revolutions, a two-stroke engine generates work with every revolution. Thus, for the same mean effective pressure (MEP), a two-stroke engine theoretically produces twice the power. This relationship can be expressed as:

$$BP = \frac{\text{bmep} \times V_d \times N}{x \times 60} \tag{8}$$

where $x = 1$ for a two-stroke engine and $x = 2$ for a four-stroke engine.

However, actually, a two-stroke engine typically achieves a lower indicated mean effective pressure (IMEP) for different reasons. First, the air exchange process occurs within a single revolution, meaning a portion of the displacement volume is dedicated to scavenging rather than compression or expansion. During this process, both the intake and exhaust ports remain

open, preventing effective compression and expansion. So, it is important to distinguish between the geometric compression ratio and the effective compression ratio.

Another limiting factor is the scavenging process, which affects the amount of fresh air which enter the engine. Unlike in a four-stroke engine, where the piston movement actively drives air and exhaust gas displacement, a two-stroke engine relies on gas flow dynamics within the cylinder. Consequently, scavenging requires pressurized intake air to properly replace the exhaust gases.

There are different scavenging methods used in two-stroke engines:

- **Cross scavenging** – This method uses an intake port and an exhaust port, with a deflector on the piston that directs the fresh air toward the top of the cylinder, pushing the exhaust gases toward the exhaust port. It represents a simpler and more cost-effective method, mainly used in small engines.
- **Loop scavenging** – In this case both intake and exhaust port are on the same side, the fresh air is pushed against the opposite wall, later the incoming charge flows make a loop and flow toward the exhaust port. it s a more efficient alternative to cross scavenging, directing the fresh charge in a circular motion to enhance cylinder filling.
- **Uniflow scavenging** – Commonly used in large diesel engines, this method employs an exhaust valve in the cylinder head and intake ports near the bottom of the cylinder. Although it increases complexity and cost, it allows better control over exhaust valve timing, enabling higher pressures and improved power output.

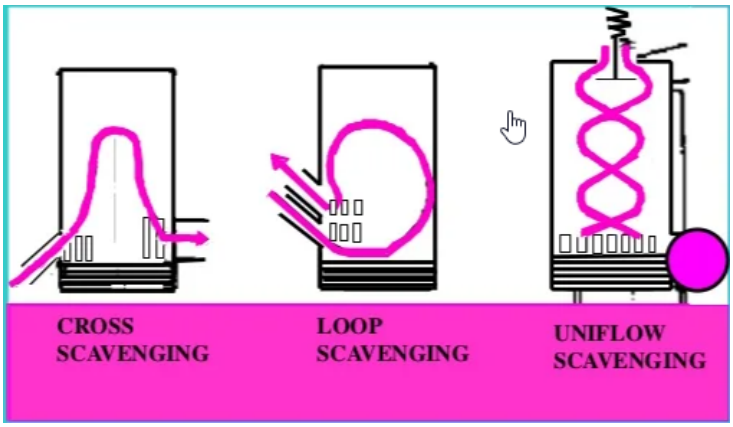

Figure 4: scavenging systems [5]

2.3 Turbocharger

The turbocharger is used to increase the pressure of the intake air and, consequently, improve the engine efficiency. It consists of a coupling between a compressor and a turbine. The turbine converts the energy from the exhaust gases into rotary motion, which powers the compressor.

For proper operation, the power output of the turbine must match the power requirement of the compressor.

$$P_c = \dot{m}_c \cdot c_p \cdot T_1 \cdot Y_c / \eta_c \tag{9}$$

$$P_t = \dot{m}_t \cdot c_p' \cdot T_5 \cdot Y_t \cdot \eta_t \tag{10}$$

$$P_c = P_t \cdot \eta_m \tag{11}$$

where:

- $Y_c = \left(\left(\frac{p_2}{p_1} \right)^{\frac{\gamma-1}{\gamma}} - 1 \right)$

- $Y_t = \left(1 - \left(\frac{p_6}{p_5}\right)^{\frac{\gamma'-1}{\gamma'}}\right)$
- p_1 is the compressor inlet pressure
- p_2 is the compressor outlet pressure
- p_5 is the turbine inlet pressure
- p_6 is the turbine outlet pressure

In diesel engines, the turbine mass flow rate is typically higher than that of the compressor due to the additional mass introduced by the injected diesel fuel. To control the turbine power output—and thus regulate the intake pressure a Turbine bypass is sometimes included in the system so:

$$\dot{m}_t = \dot{m}_a + \dot{m}_f - \dot{m}_{\text{waste\_gate}} \tag{12}$$

By combining equations (2), (3), and (4), the compressor pressure ratio can be written as:

$$\frac{p_2}{p_1} = \left[1 + \frac{\eta_c \cdot \eta_t \cdot \eta_m \cdot T_5 \cdot \dot{m}_t \cdot c'_p}{T_1 \cdot \dot{m}_c \cdot c_p} \cdot \left(1 - \left(\frac{p_6}{p_5}\right)^{\frac{\gamma'-1}{\gamma'}}\right)\right]^{\frac{\gamma}{\gamma-1}} \tag{13}$$

After compressing the intake air with the compressor, the intake air becomes hot. For this reason, an intercooler is installed at the compressor outlet to reduce the temperature of the air before it enters the intake manifold. A common factor used to describe the cooling process is the effectivness , it represent the ratio between actual temperature drop and the max possible temperature drop:

$$\alpha = \frac{T_{\text{comp\_out}} - T_{\text{engine\_in}}}{T_{\text{comp\_out}} - T_{\text{coolant}}} \tag{14}$$

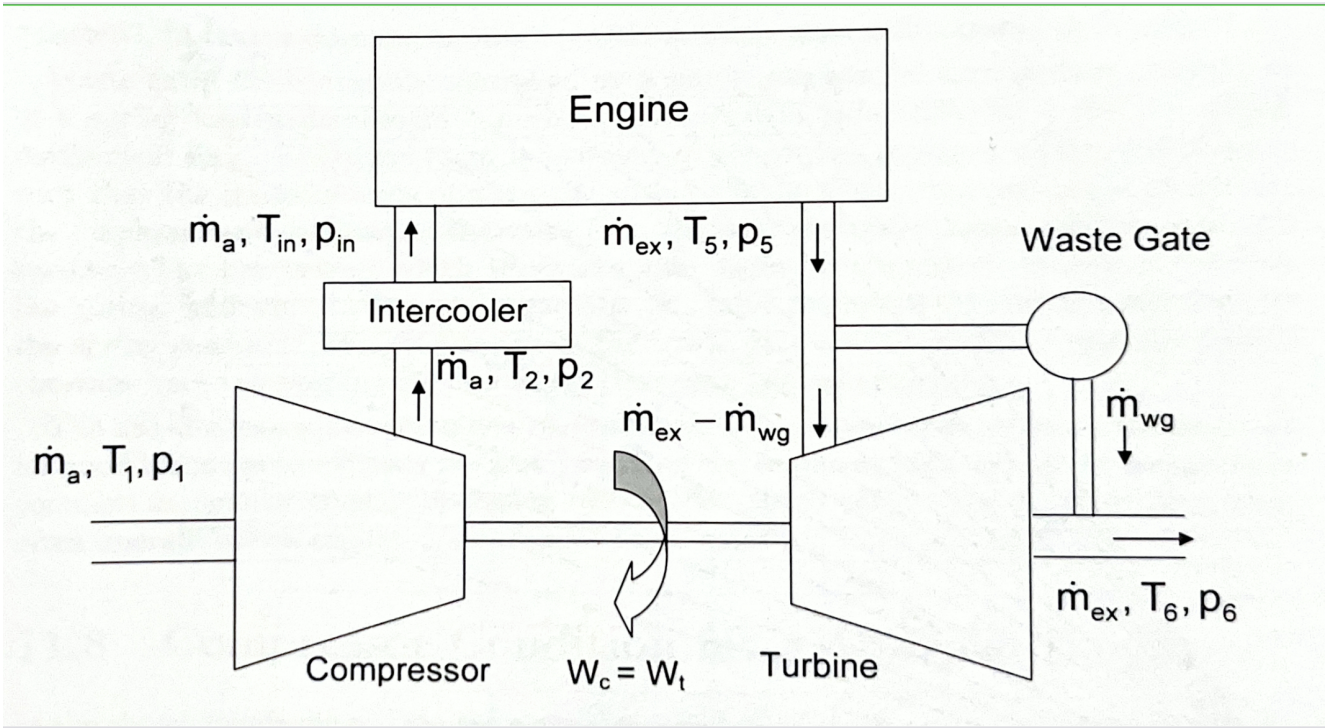

Figure 5: Scheme turbocharger layout [6]

2.4 Heat release shape of a CI engine

The combustion process of a direct injection (DI) engine can be characterized by four main phases:

1. **Ignition delay period**: This is the phase during which the injected liquid fuel evaporates and mixes with the available air. During this period, a negative heat release can be observed in the heat release rate (HRR) curve due to the heat absorbed from the air for fuel vaporization.

2. **Premixed combustion phase**: This phase occurs when the fuel-air mixture, prepared during the ignition delay, burns rapidly. This leads to a sharp rise in the heat release rate. The mixture is initially very rich, but as the available oxygen is consumed, the heat release rate decreases rapidly. However, the temperature remains high enough to allow the formation of a diffusion flame.

3. **Mixing-controlled combustion phase**: In this period, the heat release rate is significantly lower and is primarily governed by the diffusion flame, where fuel and air mix progressively before combustion occurs.

4. **Late combustion phase**: This final phase involves the burning of any remaining fuel, contributing to the completion of the combustion process.

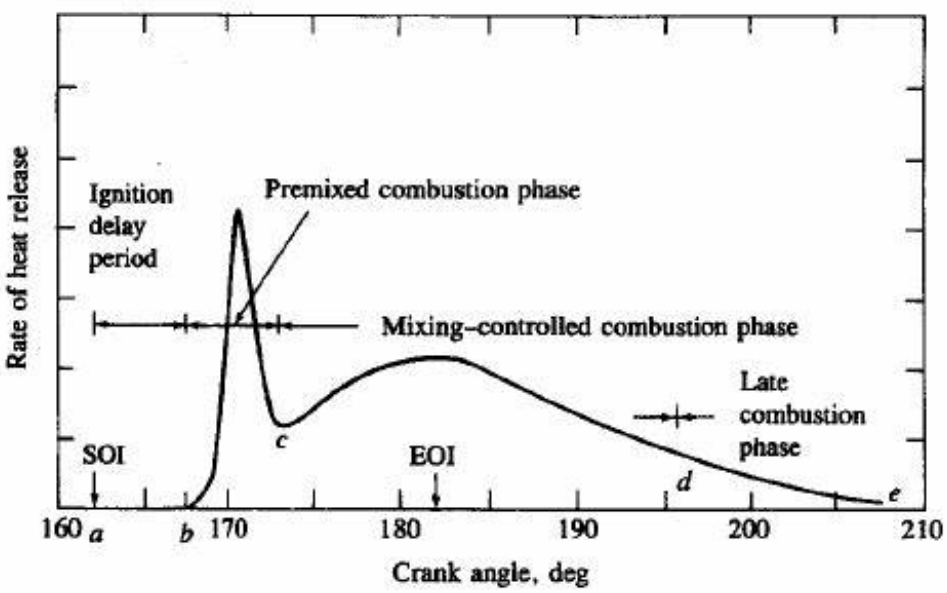

Figure 6: Heat release phases in diesel combustion [7]

2.5 Fuels

For different types of combustion, fuels require specific characteristics.

In a spark ignition (SI) engine, the fuel must be volatile enough to evaporate easily and resistant to premature ignition when mixed with air. This resistance to autoignition is known as knock resistance, which is crucial for proper engine operation.

Conversely, in a compression ignition (CI) engine, the ideal fuel must ignite rapidly when exposed to high pressure and temperature. This means that diesel and spark-ignition engines have opposite ignition requirements.

The ignition quality of fuels is measured using two primary fuel standards:

- Octane number (for SI engines)
- Cetane number (for CI engines)

To determine the octane number, two main rating tests are conducted:

1. Research Octane Number (RON)
2. Motor Octane Number (MON)

Typically, a high cetane number corresponds to a low octane number.
A key factor influencing knock resistance is fuel composition:

- Small molecules tend to resist autoignition, improving knock resistance.
- Long, straight-chain molecules have lower knock resistance and ignite more easily.
- Unsaturated carbon-carbon bonds reduce knock resistance.
- Cyclic structures stabilize the molecule and enhance knock resistance.

2.6 Emissions

The exhaust air pollutants from the engine are as follows:

- Carbon monoxide (CO): This is a dangerous gas for human life, as it is toxic when inhaled in high concentrations.
- Unburned hydrocarbons (UHC): These are partially burned or unburned fuel components. The most serious air pollution problem from these compounds arises from their reaction with O_2 or N_2, forming photochemical smog. This smog can irritate the eyes and respiratory systems.
- Oxides of nitrogen (NO and NO_2): These are very strong greenhouse gases that contribute to global warming.
- Particulate matter (PM): PM produced by the engine usually contains a significant amount of aromatic compounds, many of which are carcinogenic.

In addition, carbon dioxide (CO_2) is a major concern regarding global warming. It can only be reduced by decreasing fuel consumption.

In diesel engines, CO and UHC emissions are typically low because of the lean mixture operation. Since the fuel is not premixed with air in the combustion system, there is no presence of fuel in the crevice volume. However, there is a higher presence of NO_x emissions and PM.

The formation of PM is primarily due to the soot of solid carbon formed inside the diffusion flame. Soot formation increases as the mixture becomes richer. Raising the temperature of combustion reduces the tendency to form soot, while NO_x is formed at temperatures that allow the burning of soot.

2.6.1 Emission control

The emissions in a Compression Ignition (CI) engine can be reduced by increasing the injection pressure. This process breaks the fuel into smaller droplets, improving the mixing with air, which leads to a leaner mixture and thus less soot formation. Additionally, this reduces the ignition delay, providing lower temperature and pressure rise rates, which results in less NO_x formation.

Another solution is to apply a pilot injection, where a small amount of fuel is injected first to initiate combustion, followed by the injection of the remaining fuel. This reduces the intensity of the initial combustion, resulting in lower temperatures.

Exhaust Gas Recirculation (EGR) is another method used to reduce NO_x emissions. In an EGR system, a portion of the exhaust gases is recirculated back into the intake air. This dilutes the air-fuel mixture with inert exhaust products, which lowers the local flame temperature, thereby reducing NO_x formation.

Selective Catalytic Reduction (SCR): This system involves adding a reducing agent, such as urea, to the exhaust gases. The urea reacts with NO_x in the presence of a catalyst to convert it into nitrogen and water. The catalyst requires a minimum operating temperature to be effective.

Diesel Particulate Filter (DPF): This device is used to filter particulate matter (PM) emissions. The most common configuration is the wall-flow filter, where exhaust gases flow through porous walls that trap the particulate matter.

3 Methodology

3.1 Simulation tool

3.1.1 GT Power

The simulations in this study were carried out using GT-Power [3], a software commonly used by engine manufacturers for analyzing engine performance. GT-Power is based on 1D modeling and includes predictive combustion models, which help in studying combustion in the engine with good accuracy. Another useful feature is the possibility to include control systems, like PID controllers, to manage important engine parameters during the simulation.

Thanks to these tools, GT-Power makes it possible to simulate the behavior of the full engine, not just individual parts. This allows for a detailed analysis while also saving time, which makes it particularly suitable for the type of investigations done in this work

3.1.2 Simulation model

The G95 engine is equipped with a turbocharging system, exhaust gas recirculation (EGR), and several control systems. Additionally, the engine cylinders incorporate a predictive combustion model, a heat release model, a flow model, and models for emissions and scavenging.

The main components of the engine model, as illustrated in Figure 7, are listed below:

1. Cylinders (9) – Connected to the cranktrain, each cylinder is equipped with six injectors.
2. Injectors (6 per cylinder) – Three for diesel injection and three for methane injection.
3. Exhaust Valve – Allows combustion gases to exit the cylinder.
4. Turbine (2) – Driven by exhaust gases and mechanically connected to the compressor shaft.
5. Compressor (2) – Pressurizes intake air before it enters the cylinders.
6. Intercooler (2) – Cools the compressed air between the compressor and the intake ports.
7. Intake Ports – Deliver the cooled and compressed air into the cylinders.
8. Exhaust Gas Recirculation (EGR) System – A portion of the exhaust gases is cooled and redirected to the intake manifold using two blowers.
9. Pmax Control System – Adjusts the Start of Injection (SOI) to regulate the maximum in-cylinder pressure.
10. Pcomp Control System – Controls the Exhaust Valve Closing (EVC) timing to achieve the desired effective compression ratio.
11. IMEP Control System – Regulates the quantity of injected fuel to reach the target Indicated Mean Effective Pressure (IMEP).

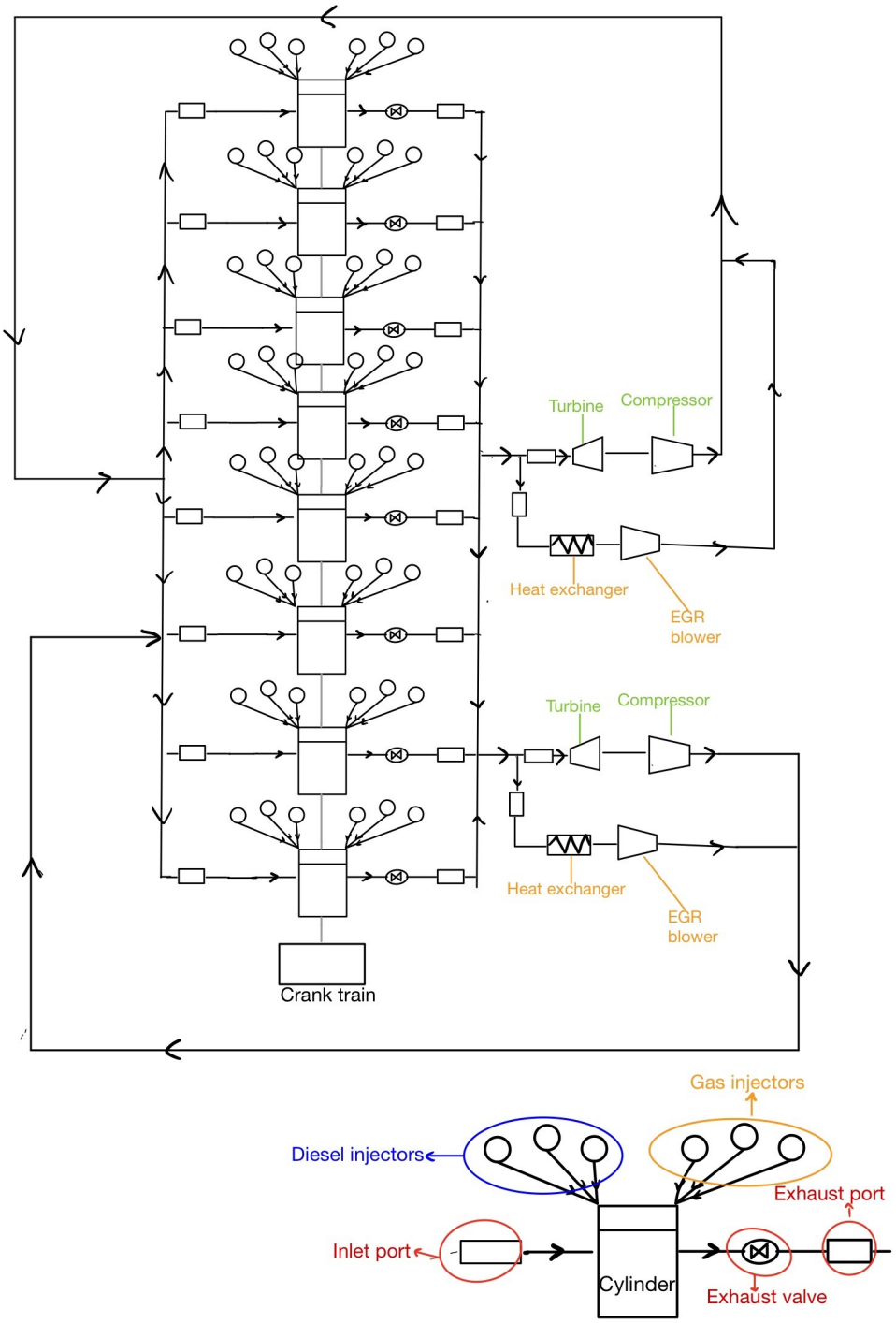

Figure 7: Simplified schematic representation of the G95 engine model

3.1.3 PID Control System Implementation

The implementation of the PID control system follows several key steps. First, all necessary components are inserted into the model. These include:

- Sensors – Are used to collect data from each cylinder.
- PID Controllers – A separate PID controller is implemented for each cylinder to allow individual regulation.
- Actuators – These components apply the control signals from the PID controllers to the corresponding engine subsystems.

All components are interconnected and integrated into the component of the model that require regulation.

The PID control system is implemented for both the diesel and gas engine models.

- Maximum cylinder pressure Control System: This PID controller regulates the maximum cylinder pressure. The controller actuator acts on the injector by modifying the SOI (Start of Injection) time. Advancing the injection increases Pmax.
- Motoring cylinder pressure Control System: This controller regulates the motoring pressure. The actuator acts on the EVC (Exhaust Valve Closing) time, and advancing the closing time increases the motoring pressure.
- IMEP Control System: This controller regulates the engine load. The actuator acts on the injector by modifying the amount of fuel injected. More fuel increases the load.
- Maximum injection pressure Control System: This controller regulates the maximum injection pressure. The actuator acts on the injector by changing the injection duration in order to maintain the same pressure. Lower duration increases the injection pressure.

3.1.4 Model limitations

The model has been calibrated by MAN Energy Solutions to predict combustion with a high level of accuracy, but there are still some limitations. One such limitation involves the injector system. Despite considering the effects of jet interactions between the nozzle and injectors during the calibration procedure, the simulation in GT Power does not account for this phenomenon. As a result, changes in the diameter or the number of holes in the injector may lead to less accurate results becuase GT Power does not capture the jet to jet interactions.

3.2 Procedure

The first requirement for performing the simulations is to implement the necessary PID controllers (for more info about PID controllers see 3.1.3) in the GT-Power model. These controllers are essential for simulating the engine under the correct conditions and ensuring proper control. In the initial phase of the study, PID controllers for Pmax, Pcomp, IMEP, and maximum injection pressure were implemented.

Once the model behaves correctly and meets all constraints, it is ready for simulation.

3.3 Model validation

In this section, the results of the simulated models are compared with the ones from the tests. The comparison focuses primarily on the in-cylinder pressure traces obtained from both simulation and test.

Additionally, several normalized parameters listed in Table 5 are used to compare simulation and experimental results

The analysis is carried out for both the conventional Diesel model and the Dual-Fuel model, which uses a Diesel pilot with methane as the main fuel.

The comparison covers four engine operating conditions: full load (100%), and partial loads of 85%, 75%, and 50% for the diesel angine, and 5 engine operating conditions for the Dual Fuel one (in which the load is varied from 100% to 75%)

The trends of each parameter listed in Table 5 that can be found in the Appendix 10.1.

Figure 8 shows that, for each operating condition, the pressure profile from the Diesel simulation model matches very well with the experimental data.

Table 5: Model parameters compared with the tested values

Compared Parameters
Brake Power
RPM
BMEP
SFOC
Air Mass Flow
Fuel Mass Flow
Scavenge Pressure
Exhaust Temp
Exhaust Pressure
Cylinder Pressure
Turbo Speed
Turbine Inlet Temp
Compression Pressure
Scavenge Temp
Comp. Inlet Temp
Cooler Inlet Temp
Cooler Outlet Temp
NOx Emissions
Ambient Pressure
Turbine Outlet Temp

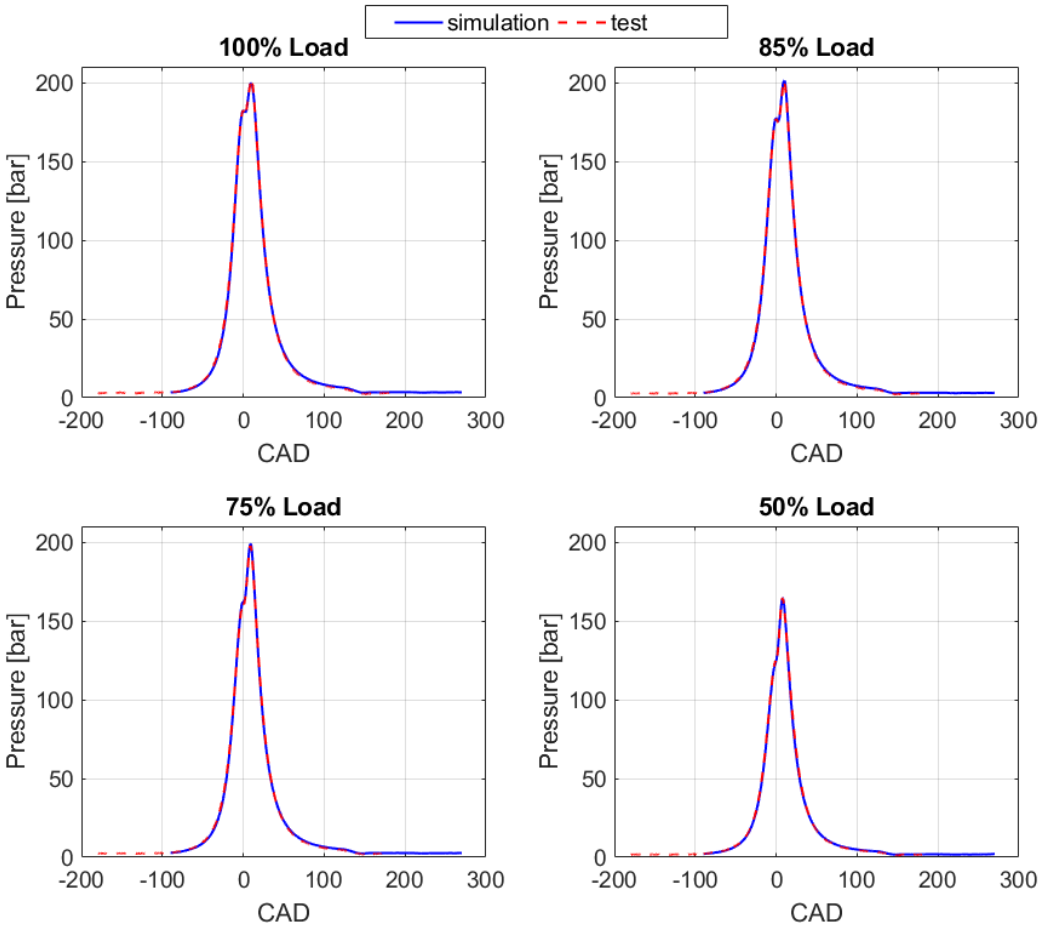

Figure 8: Pressure profiles Diesel simulaiton VS test

Figure 9 shows that, for each operating condition, the pressure profile from the Dual Fue simulation model matches very well with the experimental data.

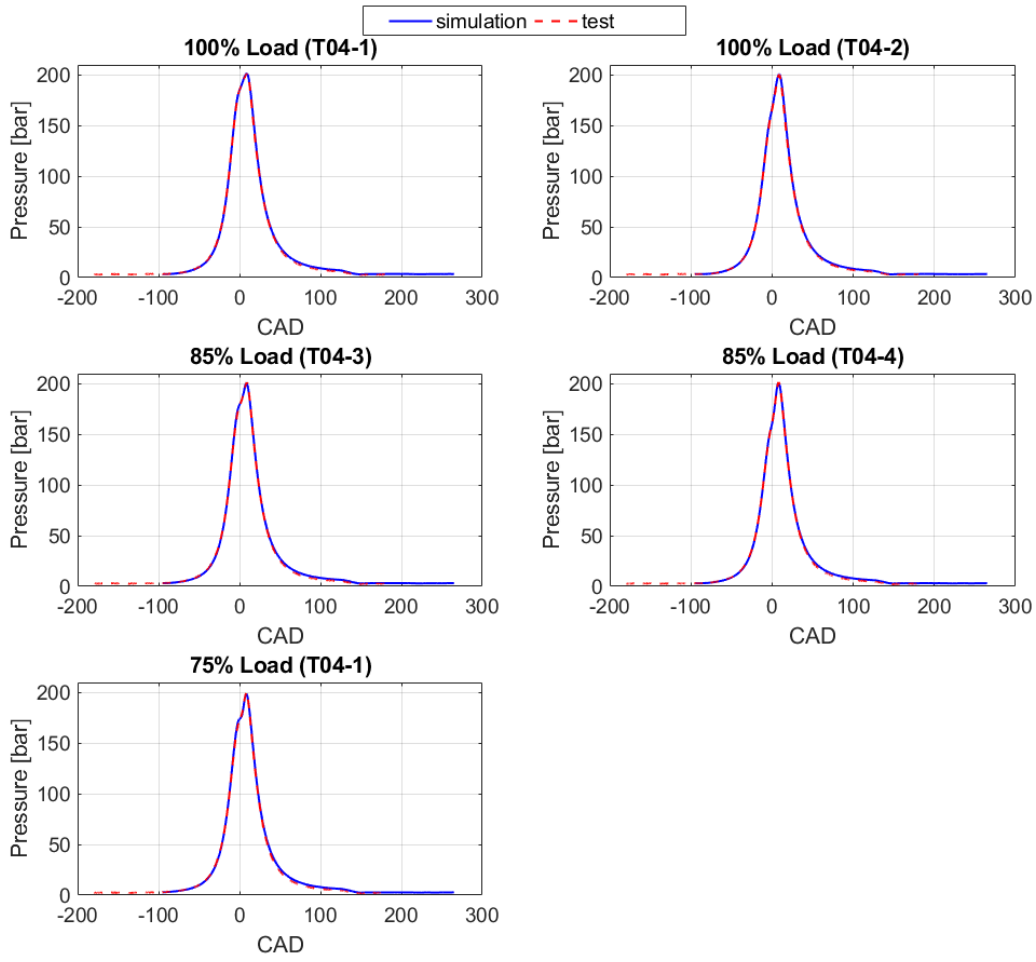

Figure 9: Pressure profiles Diesel simulaiton VS test

3.4 Simulation Approach

After having implemented the PID controllers in the model, the model is now ready for simulation. As mentioned in the Scope of Work chapter1.1, various parameters are changed. However, since many controllers were used, meaning many parameters were changed at the same time, hence it was difficult to understand the behaviour and the effect of the parameters on the combustion. To address this, initial simulations were performed without controllers, gradually increasing the number of active controllers. This step-by-step approach helps in validating the model, better understanding the combustion process, the effect of the controllers, and the impact of the changed variables.

3.5 Diesel Simulation

The simulation of the engine running on diesel is divided into two parts. The first part involves running the model with all the controllers active. In this case, the parameters analyzed are the following:

- Number of nozzle holes
- Nozzle hole diameter

- EGR level (by changing the blower speed)
- Geometric compression ratio (by changing the shims thickness)

As part of this first simulation, the results are analyzed, and other simulations are performed by combining additional parameters modification, such as combining EGR with the geometric compression ratio variation.

In the second part of the simulation, the engine run under less constrained conditions (Without one or more controller). The first step is to work with a fixed Pcomp (163 bar) and increase Pmax until 219 bar. Pmax is the maximum cylinder pressure , while Pcomp is the compression pressure, the second step involves working with a fixed maximum pressure while changing the compression pressure, which is done by changing the EVC (Exhaust Valve Closing) time. The third step is to work with a fixed Pmax-Pcomp difference and increase Pmax until 219 bar.

3.5.1 Diesel: Control on simulation

During the simulation with all the controllers on, the engine is simulated by varying different parameters as explained before. The table 6 shows standard conditions and the parameter changed for each case.

Table 6: Summary of Standard Conditions and Parameter Variations for Simulations

Standard Conditions					
Hole diameter [mm]	# of holes [-]	EGR [%]	Injection duration [CAD]	Geometric CR [-]	
1.7	5	18.7	11.83	29.5	
Case	**Varied Parameter**	**Values**			
1	Hole diameter [mm]	[1.4 - 1.5 - 1.6 - 1.7 - 1.8 - 1.9 - 2]			
2	# of holes [-]	[3 - 4 - 5]			
3	EGR [%]	[0 - 11.5 - 18.7 - 24]			
4	Geometric CR [-]	[21 - 23 - 25 - 27 - 29.5 - 31 - 33]			

In the case 1: the injector holes diameters are varied from a minimum value of 1.4 mm to a maximum value of 2 mm. In this case many simulations are made to study the effect of this parameter and optimize the enigne.

In the case 2: the number of the injector holes are changed from a minimum value of 3 to a maximum value of 5, specifically 3 simulations have been made for 3 4 and 5 holes, No additional holes were considered, becuase the injector would not be realistic.

In the case 3: the EGR level is varied from an almost null value to a maximum of 24%, which corresponds to the maximum achievable value in the model. The EGR level is computed using the average oxygen mole concentration in the pipe that collects both the compressed air and exhaust gases. The EGR percentage is then calculated using the following formula which does not match the theoretical one. In fact, in the theoretical expression, the denominator should include the oxygen mole fraction in the exhaust gases, while here it refers to the fresh air:

$$\text{EGR } \% = \frac{\text{mean}(X_{O_2})}{X_{O_2,\text{air}}} \times 100$$

Where:

- (X_{O_2}) represents the oxygen mole concentration in the intake pipe, which varies as a function of CAD.
- $X_{O_2,\text{air}}$ is the theoretical oxygen mole fraction in fresh air, with a typical value of 0.21.

In the case 4: the geometric compression ratio is varied from a minimum value of 23 to a maximum of 33. The geometric compression ratio is adjusted by changing the thickness of the shims. In the model, this change is implemented by modifying two parameters: the geometric compression ratio and the distance from TDC (Top Dead Center) to the opening of the scavenging ports. In this case, many simulations have been performed in order to find the optimum value.

3.5.2 Diesel: Control off simulation

During the simulation with some controllers off, the engine is simulated by varying different parameters as explained before. The Table 7. shows the parameters changed for each case. In this simulation, 3 more cases were run by turning off one or more controllers.

Case	**Sweep Variable**	**P_{max} [bar]**	**P_{comp} [bar]**	**P_{max}-P_{comp} [bar]**
5	P_{max}	[199:219]	163	variable
6	P_{comp}	199	[153:173]	variable
7	P_{max} P_{comp}	[199:219]	[163:183]	36

Table 7: Parameters variation for unconstrained diesel simulations.

In the case 5: Pmax is varied from 199 bar (standard condition) up to 219 bar, while Pcomp is kept fix to 163 bar.

In the case 6: Pcomp is varied from 153 bar to 173 bar while Pmax is kept fix to 199 bar, in order to evaluate the effect on the combustion considering all the other cosntraints on .

In the case 7: Pmax is varied from 199 bar (standard condition) up to 219 bar, at the same time also Pcomp is changed in order to have the difference Pmax-Pcomp=36 bar.

In order to change Pmax (maximum cylinder pressure) the start of injection is varied, while in order to change Pcomp (compression pressure) the EVC (exhaust valve closing) time is changed.

3.6 Dual fuel (Diesel pilot and Methane injection) Simulation

The Dual Fuel simulation as the diesel one is divided in 2 parts. The first part involve running the model with all controllers activated. The parameters analyzed are as follows:

- Number of nozzle holes (gas)
- Nozzle hole diameter (gas)
- EGR level (by changing the blower speed)
- Geometric compression ratio (by changing the shim thickness)
- Pilot on/off
- Pilot start of injection
- Pilot injection duration
- Pilot injected mass

In the second part of the simulation, the engine is run under unconstrained conditions:

- Maximum injection pressure (Gas)
- P_{max} is varied
- P_{comp} is varied
- P_{max} is varied while maintaining a fixed P_{max} – P_{comp} difference

3.6.1 Dual fuel (Diesel pilot and Methane injection) : Control on simulation

The engine is simulated by varying the gas injector parameters, global parameters and diesel pilot parameters as explained before. The table 8 shows standard conditions and the parameter changed for each case.

Table 8: Summary of Standard Conditions and Parameter Variations for GAS Simulations

Standard Conditions					
Hole diameter (gas) [mm]	# of holes (gas) [-]	EGR [%]	Injection duration (gas) [CAD]	Geometric CR [-]	
3.5	5	17.9	7.28	29	
Pilot SOI [CAD]	Injection duration [CAD]	Pilot mass %			
-7.5	11.26	6.5			
Case	**Varied Parameter**	**Values**			
8	Hole diameter (gas) [mm]	[2.5, 3, 3.5, 4, 4.5]			
9	# of holes (gas) [-]	[3, 4, 5]			
10	EGR [%]	[0, 10.5, 17.9, 23.8]			
11	Geometric CR [-]	[25, 27, 29, 31, 33, 35, 37]			
12	Pilot on/off	[on, off]			
13	Pilot SOI [CAD]	[-8.5 : -5.5]			
14	Injection duration [CAD]	[2.25 : 11.26]			
15	Pilot mass %	[6.5, 13.2, 22.7, 33.8]			

Cases 8, 9, 10 and 11 of Table 8 are carried out in the same manner as in the diesel case (1 2 3 4) 3.5.1. Therefore, the procedures and considerations described for the diesel simulations also apply here.

In the case 12: is compared the scenario in which there is the diesel pilot injection and another one in which the pilot is removed and so only methane is injected.

In the case 13: the start of pilot injection is varied.

In the case 14: the pilot injection duration is varied. This is done without changing the maximum injection pressure, thus the diameter and number of holes of the diesel injector are adjusted

In the case 15: the pilot mass injected is varied. This is done without changing the maximum injection pressure, thus the diameter and number of holes of the diesel injector are adjusted

3.6.2 Dual fuel (Diesel pilot and Methane injection) : Control off simulation

In this case, 4 more simulations were performed by turning off one or more controllers, as shown in Table 9.

Case	**Sweep Variable**	**P_{max} [bar]**	**P_{comp} [bar]**	**P_{max}-P_{comp} [bar]**	Max injection pressure Normalized [-]
16	P_{max}	[198.5:218.5]	167.4	[31.1:51.1]	1
17	P_{max}, P_{comp}	[198.5:218.5]	[167.4:187.4]	31.1	1
18	P_{comp}	198.5	[157.4:177.4]	[41.1:21.2]	1
19	P_{inj}	198.5	167.4	31.1	[1:2.01]

Table 9: Initial conditions for unconstrained diesel simulations.

Cases 16, 17, and 18 of Table 9 are carried out in the same manner as in the diesel case (5 6 7). Therefore, the procedures and considerations described for the diesel simulations also apply here.

In the case 19 of Table 9 the maximum injection pressure of the gas injector is changed, specifically the standard value increases up to its 101%.

3.7 Collected results

The GT Power interface provides both the simulation status and the results. Various output files are generated to collect all the necessary variables required for the study. GT Power provides different kinds of data, but the two most important categories for this study are "Plot Data" and "Case Data". The "Plot Data" consists of results expressed as a function of Crank Angle Degree

(CAD), and these are represented as vectors. On the other hand, the "Case Data" includes average values or single values, representing scalar quantities.

The data collected includes:

- **Plot data (from cylinder #1):**
  - Apparent Gross Heat Release Rate (HRR)
  - Cylinder pressure
  - Injection pressure
  - X_{O_2}
- **Case data (from cylinder #1):**
  - Start of combustion
  - CA50
  - 10–90% combustion duration
  - Lambda
- **Case data (from injector #1):**
  - Start of injection
  - Injected mass
  - Maximum injection pressure
- **Case data (from engine):**
  - SFOC
  - NOx

The in-cylinder data are collected from cylinder #1 rather than using the average between the 9 cylinders, this becuase the difference is minimal, infact by looking at the IMEP, is observed a variation between cylinder #1 and the average cylinder of 0.004% for the diesel model and 0.0003% for the Dual Fuel model.

Of course, sometimes other parameters are also important to visualize and analyze, such as cylinder temperature, valve temperature, cumulative heat losses, and scavenging pressure. These variables can provide valuable insight into the results, especially when certain behaviors become less predictable due to the influence of the control systems. However, the variables listed above are the ones most frequently used in the charts and throughout the analysis.

3.8 Heat Release Analysis

The heat release analysis is conducted in the Diesel simulation to provide insights into the amount of premixed energy , which results in better performance, such as achieving the lowest fuel consumption or minimizing NOx emissions.

To perform this analysis for the Diesel results, a Wiebe function fit is applied to different HRR profiles. The HRR profiles considered for this analysis are those obtained from the variation of the number of injector holes and the variation of the EGR (Exhaust Gas Recirculation) levels.

Once the Wiebe function is well-fitted, the premixed energy is computed by integrating the Wiebe function profile, more details can be found in the appendix 10.

4 Results: Diesel control on

In this section, the results of the engine running on diesel with all PID control systems active (IMEP control, Pmax control, Pcomp control, and maximum injection pressure control) are presented.

4.1 Nozzle diameter and Number of nozzle holes variation

Changing the nozzle diameter or the number of nozzle holes affects the flow area.

$$\text{flow\_area} = \frac{\pi \cdot n_h \cdot d^2}{4} \tag{15}$$

where:

- n_h = number of nozzle holes
- d = nozzle hole diameter

Without any controller turned on, reducing the diameter or number of holes increases the injection pressure. Consequently, the maximum cylinder pressure would also increase, leading to lower fuel consumption. However, with all controllers active, the effect of changing the flow area can be observed in Figure 10 (in which the hole diameter is changed from 1.4 mm up to 2 mm). To maintain a fixed maximum injection pressure, the injection duration changes. Reducing the hole diameter means increasing the injection duration. The increased injection duration leads to slower combustion; in fact, the width of the heat release rate (HRR) increases with a reduced diameter. Due to the slower combustion, the start of injection (SOI) is advanced to reach the target maximum pressure.

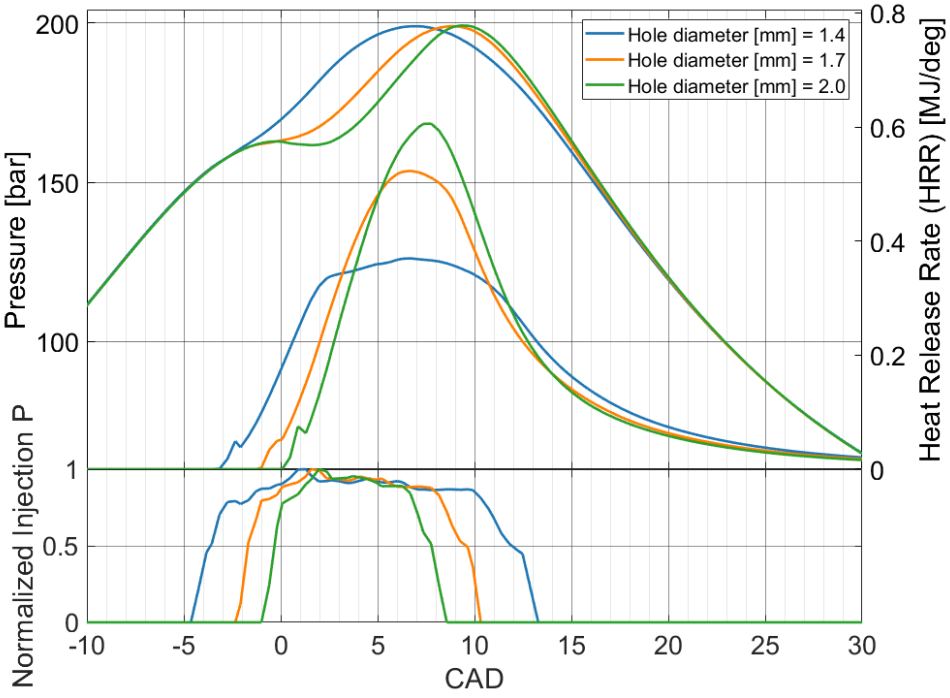

Figure 10: Hole diameter variation, HRR P vs CAD

Changing the number of nozzle holes also affects the flow area; therefore, the results shown in Figure 11 are similar to those observed when the hole diameter was varied 4.1. .

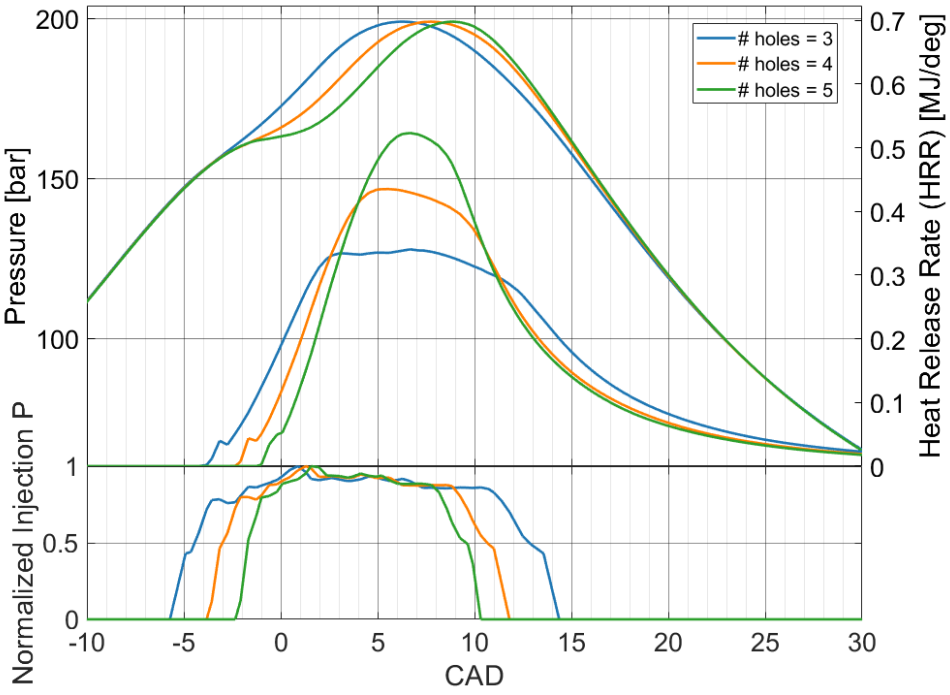

Figure 11: Number of nozzle holes variation, HRR P vs CAD

The results in terms of fuel consumptions when varying the mass flow area are shown in Fig. 12. Two curves are presented: the blue line corresponds to variations in flow area by changing the number of nozzle holes, while the red line represents variations obtained by changing the hole diameter. The green dot indicates the reference case (5 holes with diameters of 1.7mm), It can be noticed that reducing the flow area can actually bring some benefits, but only if this is done by decreasing the hole diameter. Reducing the diameter from 1.7 mm to 1.6 mm results in a small reduction in SFOC, around 0.05% (Yellow dot). This small improvement is likely due to the longer injection duration caused by the smaller diameter, which leads to a slower HRR. This, in turn, allows the injection to be slightly advanced so that the peak pressure occurs slightly closer to TDC.

On the other hand, reducing the flow area by decreasing the number of holes does not yield the same benefit. For instance, if we compare two injectors with nearly the same total flow area (approximately 9 mm^2) one with 4 holes of 1.7 mm and the other with 5 holes of 1.5 mm there is still a noticeable difference in SFOC.

This suggests that the variation in fuel consumption is not solely due to the flow area, since it remains almost identical in both cases. Instead, the difference may be attributed to air entrainment and spray atomization characteristics. Fewer, larger holes may result in poorer fuel–air mixing, leading to less efficient combustion.

This hypothesis is consistent with the findings reported in [8], but a more detailed analysis using CFD simulations would be necessary to confirm the underlying mechanisms.

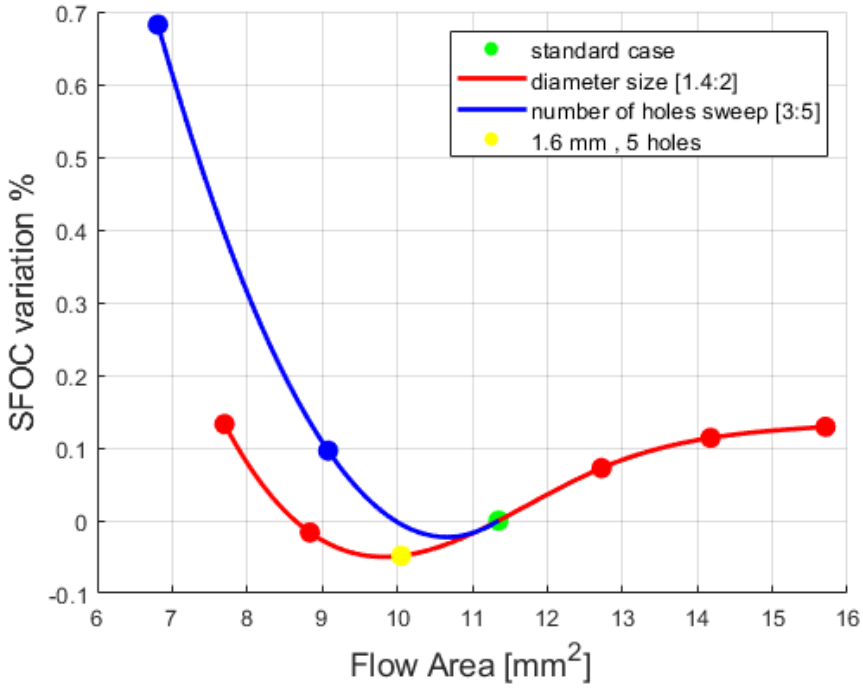

Figure 12: Normalized SFOC vs Flow area

4.2 EGR level variation

The external EGR level is varied from 0% to 24% by changing the EGR blower speed. From Figure 13, it can be noted that reducing the EGR level means retarding the SOI of diesel in order to reach the target maximum cylinder pressure.

Looking at the HRR shape, it is not easy to identify a clear trend just by observing the peak, and this is mainly influenced by the many controllers acting on the engine. However, what can be observed is that due to the delayed SOI for lower EGR levels, the SOC (start of combustion) starts later. During the premixed phase, due to the higher oxygen amount, the HRR becomes faster for low EGR levels. Still, no clear trend on the HRR peak is found.

It should also be taken into account that the amount of injected fuel changes during the variation of EGR levels. Another important consideration is that at SOI, the cylinder temperature is higher in the high-EGR-level cases. This is because, due to the control acting on the compression pressure, the EVC timing is varied. Specifically, the variation leads to an advanced closing time for high EGR levels, which reduces the time for the residual gases to leave the cylinder, resulting in a higher temperature.

So, despite the different EGR levels, it can be noted that the ignition delay for the 0% EGR case is higher, meaning it takes more time to start combustion. All of these effects help explain why it is difficult to identify a trend in the HRR peak.

However, by looking at the combustion duration (10%-90%), a trend can still be identified. As expected, lower EGR levels lead to a shorter combustion duration due to the higher oxygen content.

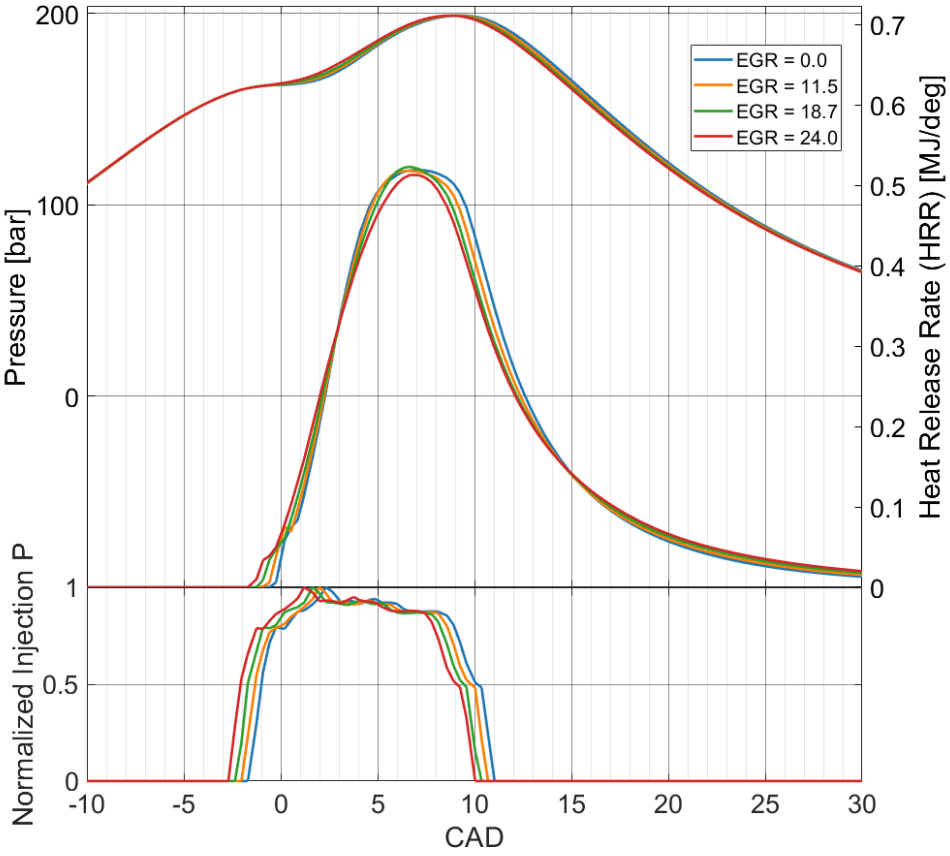

Figure 13: EGR level variation, HRR P vs CAD

For this reason, by looking at Figure 14, a clear trend in NOx emissions can still be noted: NOx decreases as the EGR level increases, while SFOC decreases as the EGR level decreases, reaching a minimum value at an EGR level of 10.5%. At 0% EGR level, SFOC is slightly higher. This can be attributed to a too-delayed combustion phase and too increased heat losses caused by the higher flame temperatures due to the higher oxygen content.

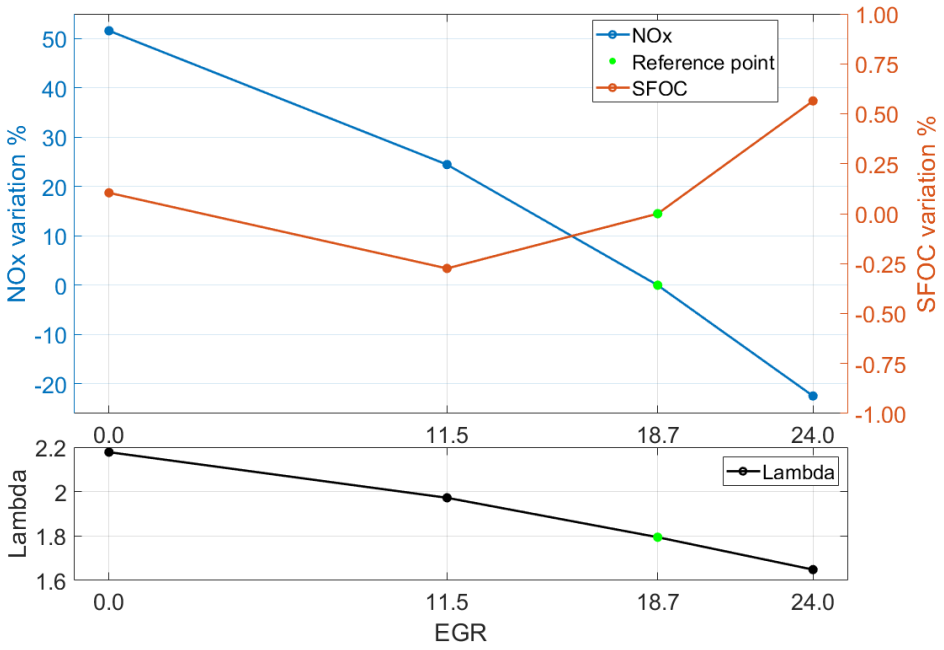

Figure 14: Normalized SFOC, NOx, Lambda vs EGR%

EGR %	0	11.5	18.72	24
Cumulative Energy Loss [MJ]	32.34	31.40	31.61	32.25
Combustion Duration [CAD]	12.4	12.99	13.63	14.24
EVC Time [CAD]	287	280	273	266

Table 10: Key parameters at different EGR levels.

4.3 Geometric compression ratio variation

In Figure 15, the effect of changing the geometric compression ratio on the heat release rate (HRR) can be observed. Specifically, increasing the geometric compression ratio delays the start of injection (SOI) in order to reach the target maximum pressure, at the same time in order to keep the compression pressure fixed to 163 bar the EVC time is delayed when the geometric compression ratio is increased, delaying the EVC time reduces the amount of trapped air in the cylinder before combustion and so the Air Fuel ratio (AF) goes down for higher geometric compression ratio as shown in Table: 11, as a consequence less oxygen is present with higher geometric compression ratio. So the effect of the higher geometric compression ratio on the HRR is counterbalanced by the lower oxygen amount inside the cylinder, this makes it difficult to identify a clear trend in the HRR peak, but can still be identified a trend in the combustion duration (10%-90%).

Geom CR [-]	23	25	29.5	34
Burn duration 10% - 90% [CAD]	13.496	13.508	13.629	13.659
AF ratio [-]	30.6	29.1	25.7	23.8

Table 11: Burn duration and AF ratio at different geometric compression ratios.

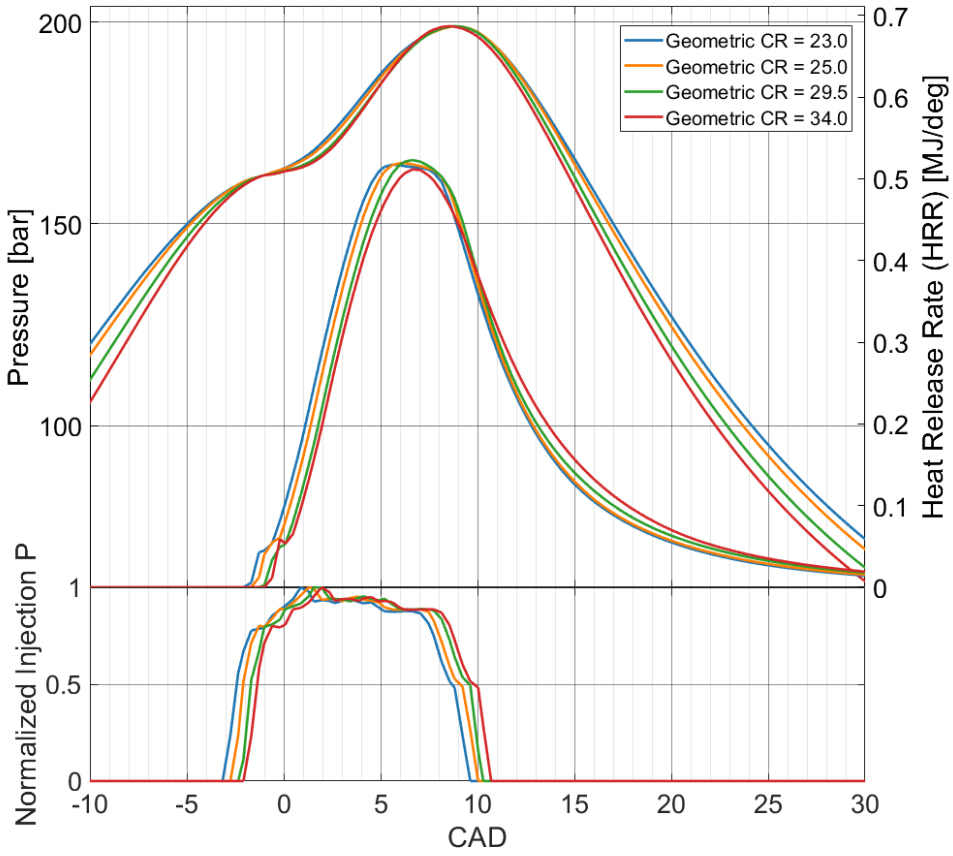

Figure 15: Geometric compression ratio variation, HRR P vs CAD

The results in terms of NOx and SFOC are shown in Fig. 16, where two curves are presented: one black and one red. They show the geometric compression ratio sweep at different EGR levels (18.7% and 11.5%), with the EGR standard condition represented by the black line. It can be observed that at an EGR level of 18.7% (black line, std case), the lowest SFOC value is achieved by increasing the geometric compression ratio from 29.5 to 31, and NOx emissions decrease as the geometric compression ratio increases this is due to the slower combustion that can be seen in the Table 11, resulting in reduction of SFOC and NOx respectively of 0.01% and 5%. For this reason, a sweep was also performed with a lower EGR level, since lower EGR increases efficiency and NOx emissions, but at the same time, increasing the geometric compression ratio reduces NOx. As a result, with an EGR level of 11.5% and a geometric compression ratio of 31, a reduction of 0.18% in SFOC is obtained, with an increase in NOx of 16%.

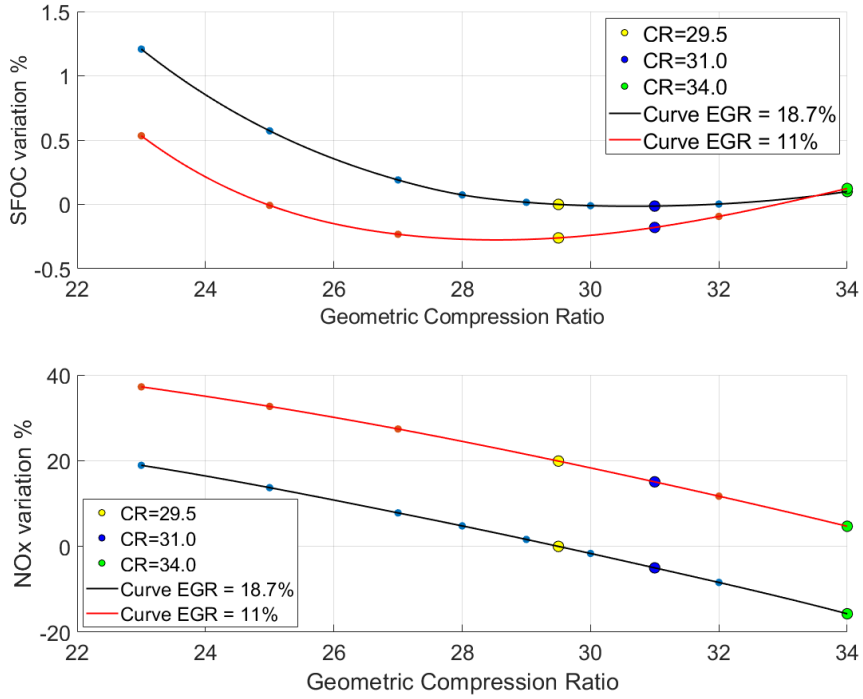

Figure 16: Geometric compression ratio variation, Normalized NOx and SFOC

4.4 Heat release analysis

Number of Holes Variation

The Heat Release Rate (HRR) obtained from each simulation with varying the numbers of nozzle holes is fitted using a Wiebe function [9]. This allows for the estimation of the premixed energy component.

As shown in Figure 17, the fit quality is satisfactory: the red curve represents the Wiebe fit, while the black curve corresponds to the simulated HRR profile. By integrating the Wiebe curve, the premixed energy is obtained.

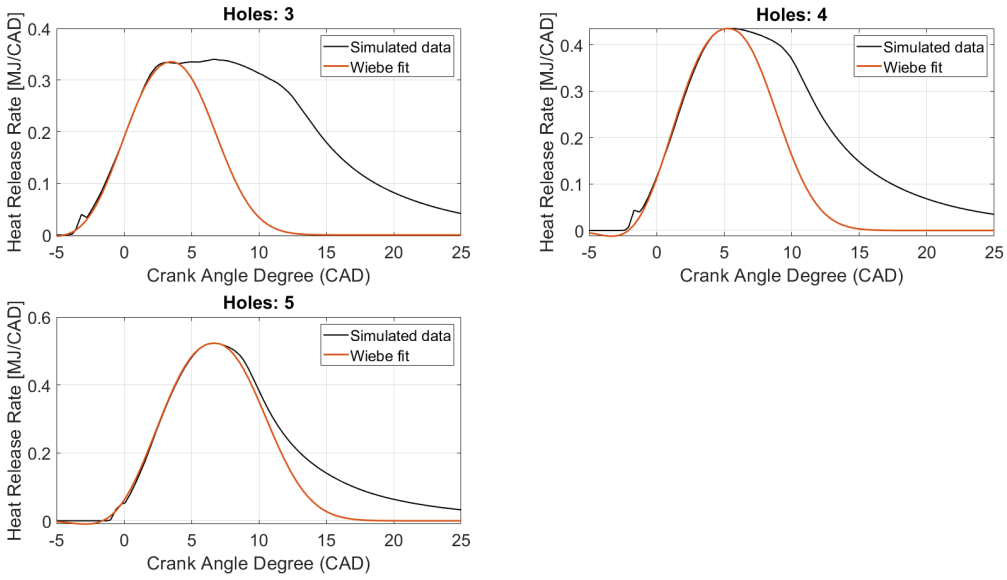

Figure 17: Wiebe fit VS simulation (number of holes case)

In Figure 18, the premixed energy is plotted against the Specific Fuel Oil Consumption (SFOC). It can be observed that increasing the premixed energy leads to a reduction in SFOC, with a minimum occurring at a premixed energy of 46.4 MJ, which corresponds to the standard configuration.

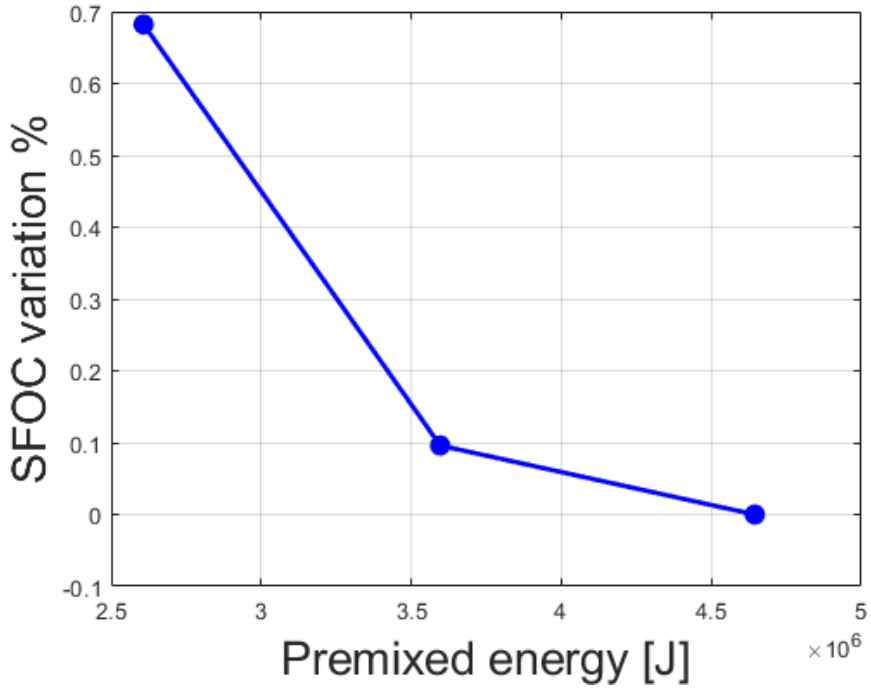

Figure 18: Normalized SFOC vs. premixed energy (number of holes variation).

EGR Level Variation

As can be seen in Fig 19 also the HRR profiles from the EGR sweep are fitted with a Wiebe function

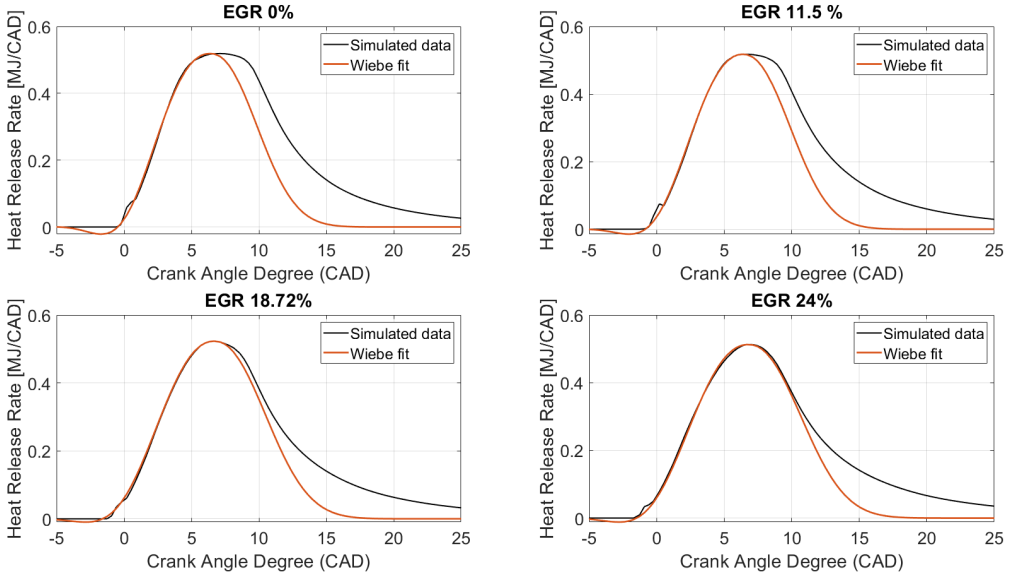

Figure 19: Wiebe fit VS simulation (EGR level case)

However, in this case, increasing the premixed energy beyond a certain point results in an

increase in SFOC, as shown in Figure 20. The optimal value is observed at a premixed energy of 42.4 MJ.

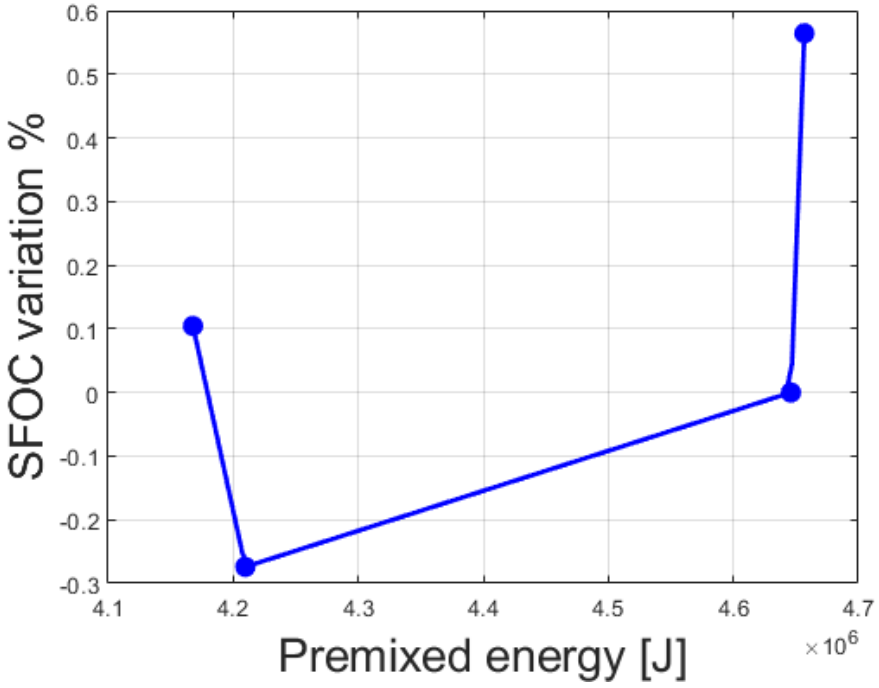

Figure 20: Normalized SFOC vs. premixed energy (EGR level variation).

Based on both analyses, the optimal range for premixed energy appears to be between 42 and 46 MJ. This result is valid for the G95 engine operating with diesel under all the constraints mentioned in Section 1.2.

5 Results: Diesel control off

In this section, the results of the engine running on Diesel with one or more PID control systems deactivated are presented.

5.1 Maximum cylinder pressure variation with a fixed P_{comp}

From Figure. 21, it can be observed that advancing the SOI from -2.03 to -3.65 CAD BTDC leads to an increase in the maximum cylinder pressure of 20 bar, while the compression pressure (P_{comp}) is kept constant at 163 bar. As a result an advanced and higher heat release rate (HRR) peak is obtained with advanced SOI; this is becuase the fuel has more time to mix with air. This shift leads to an advance and increase in the pressure peak as well.

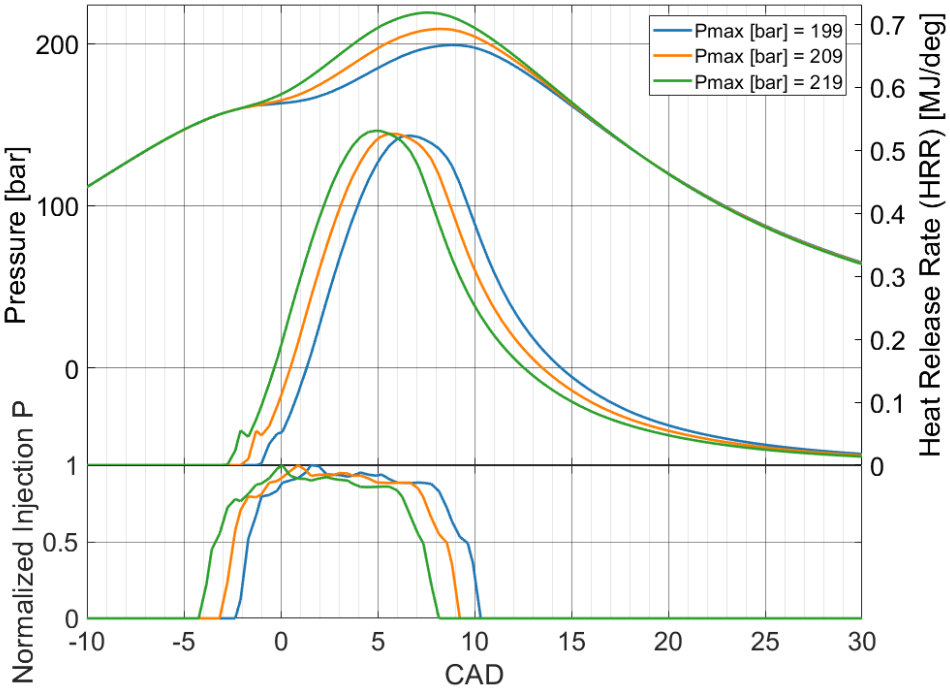

Figure 21: Pmax variation (with Pcomp fixed), HRR P vs CAD

As can be seen in Figure22, the trend of SFOC and NOx emissions is clear, SFOC decreases due to a better efficiency related to the advanced SOI which shifts the combustion closer to TDC, while NOx increases due to higher cylinder temperatures, which are also evident from the higher cylinder pressure. As a consequence, when the maximum cylinder pressure is increased from 199 bar up to 219 bar, a reduction in specific fuel oil consumption (SFOC) of 1.37% is observed, accompanied by an increase in NO_x emissions of 8.92%, while lambda does not show any significant variation because the control system regulating the maximum compression pressure is active. To maintain the same compression pressure across all cases, the exhaust valve closing (EVC) timing does not vary substantially. As a result, the amount of trapped air remains nearly constant, and consequently, λ is not significantly affected.

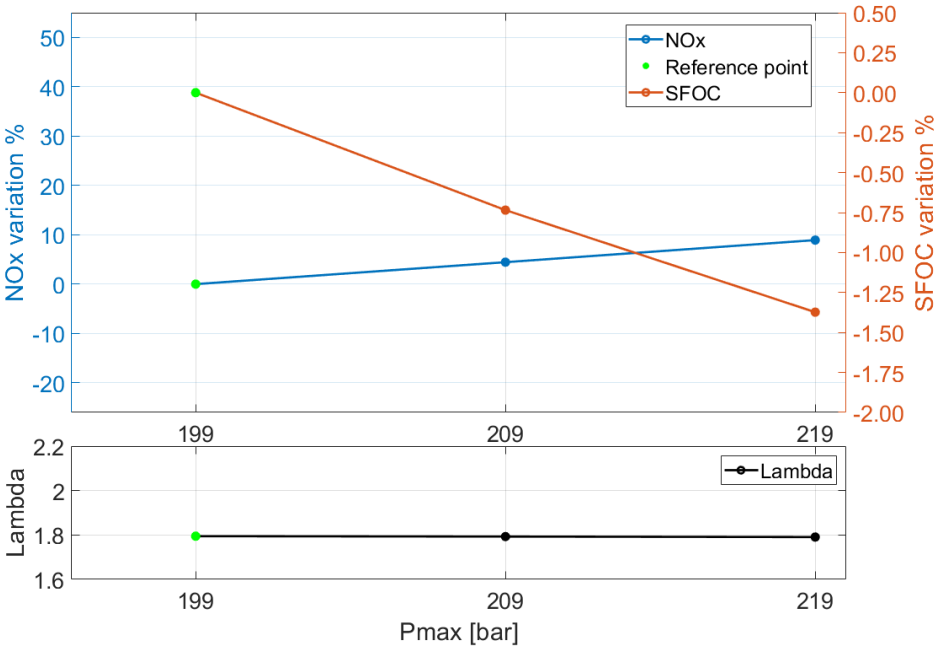

Figure 22: Pmax variation (with Pcomp fixed), Normalized SFOC NOx and lambda

5.2 Maximum cylinder pressure variation with a fixed P_{max}-P_{comp}

From Figure 23, the effect of varying the start of injection (SOI) to change the maximum cylinder pressure, and the exhaust valve closing (EVC) timing to change the compression pressure in order to keep the difference Pmax-Pcomp fixed at 36 bar, can be observed. It can be noted that, with higher pressures, the HRR peak is lower. This occurs because the injection duration is longer in order to maintain a fixed maximum injection pressure. This phenomenon happens because changes in cylinder pressure affect the injection pressure, and in this case due to the change in both peak pressure and compression pressure, the variation in cylinder pressure is not negligible. This relationship is described by the following equation:

$$\dot{m} = C_d A \sqrt{2\rho\Delta P} \quad \text{with} \quad \Delta P = P_{\text{inj}} - P_{\text{cyl}} \tag{16}$$

To maintain a constant mass flow rate, ΔP must remain constant. Therefore, if P_{cyl} increases, P_{inj} must also increase, this is valid becuase the injection pressure is not the critical one.

But due to the PID control system that regulate the maximum injection pressure, what can be seen is a growth (Table: 12) on the injection duration that slow down the combustion affecting in this case the HRR peak.

Pmax [bar]	199	209	219
Injection Duration [CAD]	11.49	11.84	12.18

Table 12: Injection duration corresponding to different maximum cylinder pressures.

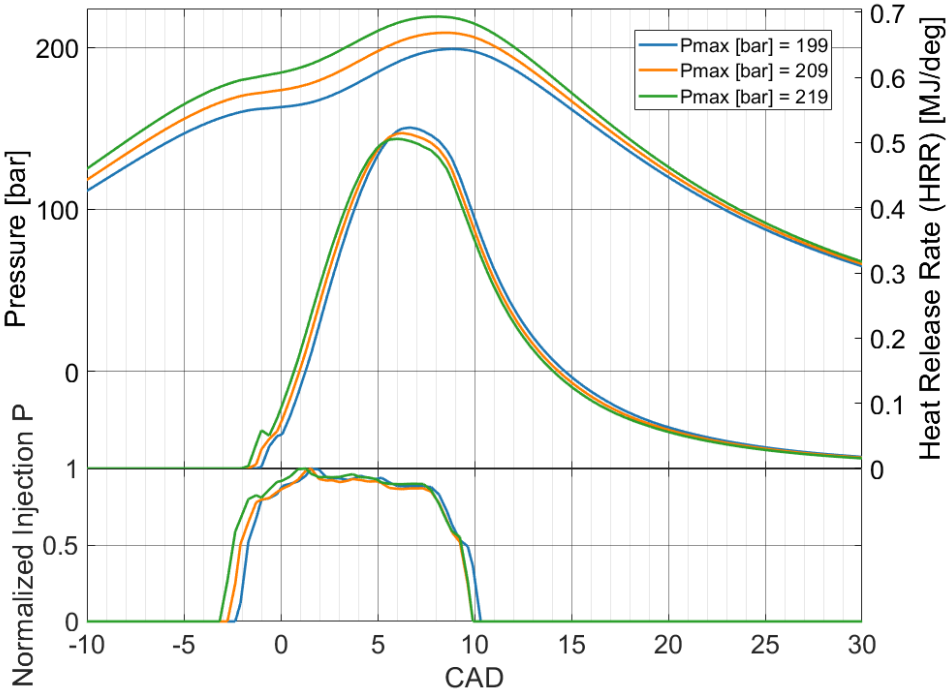

Figure 23: Pmax variation (with Pmax-Pcomp fixed), HRR P vs CAD

The effect on NOx emissions, SFOC and lambda is shown in Fig. 24. It can be seen that NOx increases with higher pressures, while SFOC decreases. This is an expected trend, as higher pressures result in higher temperatures, which are responsible for increased NOx emissions. At the same time, achieving higher pressures closer to top dead center (TDC) leads to improved efficiency. By increasing $P_{\max}$ from 199 to 219 bar, a reduction in SFOC of approximately 1.12% and an increase in NOx of about 7.36% are observed. It can also be seen that λ increases, which is related to the change in the EVC time. In fact by looking at the trapped air in the cylinder before combustion in Table 13, it can be seen that the trapped air increases when the EVC time is advanced (higher pcomp), while the injected fuel amount decreases. As a consequence the Air Fuel Ratio (AFR) increases if the EVC time is advanced, and thus a higher Lambda is observed.

P_{max} [bar]	**Normalized Trapped air [-]**	**Normalized Fuel [-]**	**AF [-]**
199	0.988	1.006	25.7
209	1	1	26.2
219	1.035	0.995	27.3

Table 13: Air-fuel data at different peak pressures

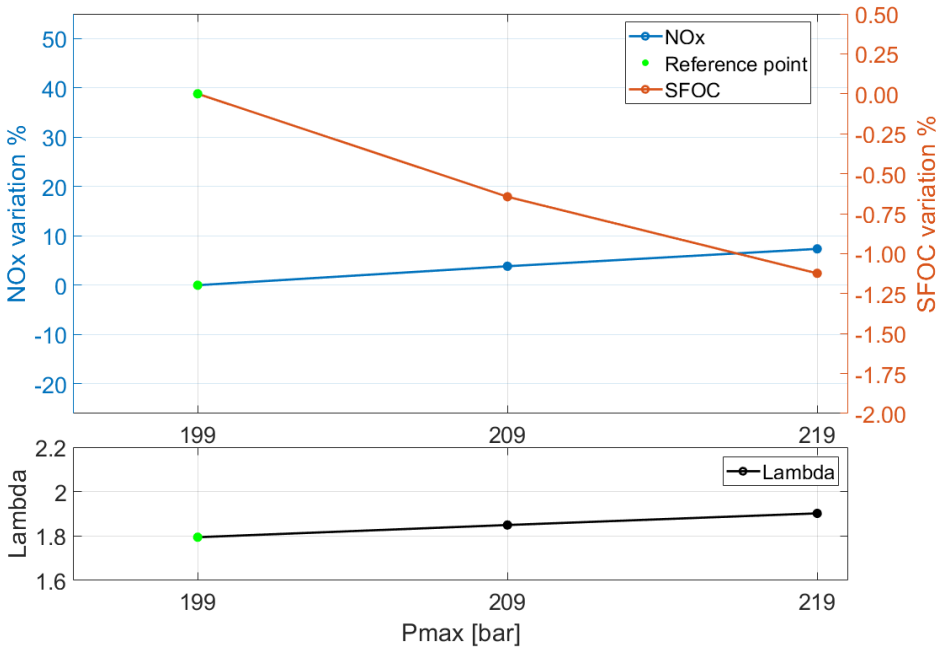

Figure 24: Pmax variation (with Pmax-Pcomp fixed), Normalized SFOC NOx and lambda

5.3 Compression pressure variation

In this case, only the Exhaust Valve Closing (EVC) timing is varied to increase or reduce the compression pressure. By maintaining a constant $P_{\max} = 199$ bar, the difference $P_{\max} - P_{\text{comp}}$ is adjusted within a range of 26 to 46 bar, as shown in Figure 25. Due to the presence of engine control systems, increasing the compression pressure (P_{comp}) causes a delay in the start of injection (SOI) to mantain the fixed $P_{\max}$. As showed in Table: 14, as the compression pressure increases, the injection duration also increases to maintain the fixed maximum injection pressure. This behavior is explained in Section 5.2. As a result, the HRR peak with higher compression pressure is lower.

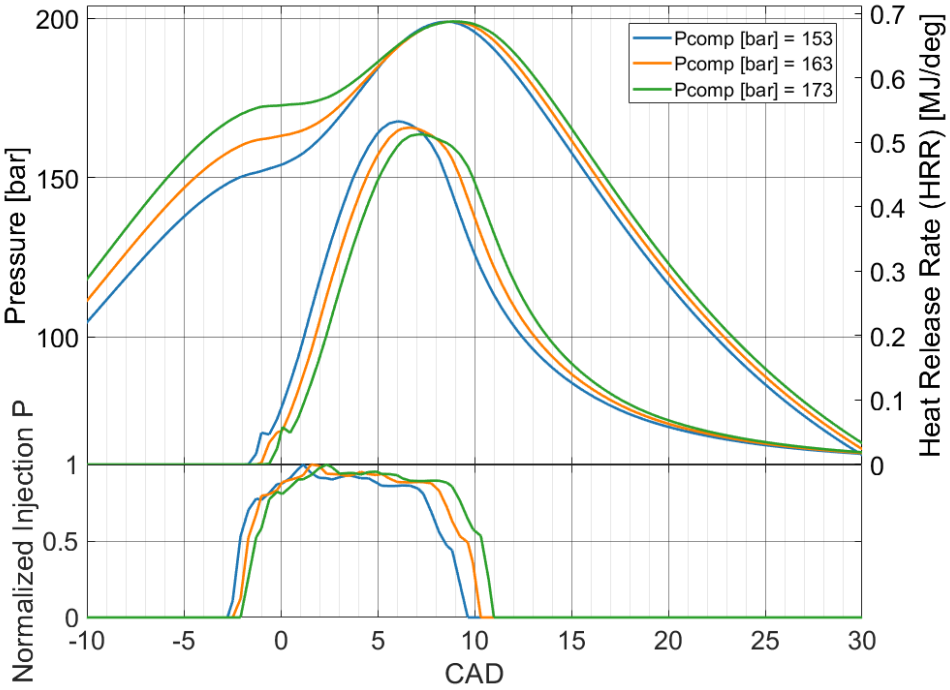

Figure 25: Compression pressure, HRR P vs CAD

Pcomp [bar]	153	163	173
Injection Duration [CAD]	11.84	12.06	12.29

Table 14: Injection duration corresponding to different compression pressures.

As seen in Figure 26, Specific Fuel Oil Consumption (SFOC) decreases with delayed EVC timing (which corresponds to lower P_{comp}). This happens because the injection duration becomes shorter, leading to a faster heat release rate (HRR). Additionally, the start of injection (SOI) is advanced, which improves thermal efficiency by advancing the cylinder pressure peak.

NO_x emissions are only slightly affected; they tend to decrease with increasing P_{comp} due to the lower HRR peak. Meanwhile, λ increases for the same reasons explained in the previous case (see Section 5.2). Table 15 shows the values of normalized trapped air and fuel injected.

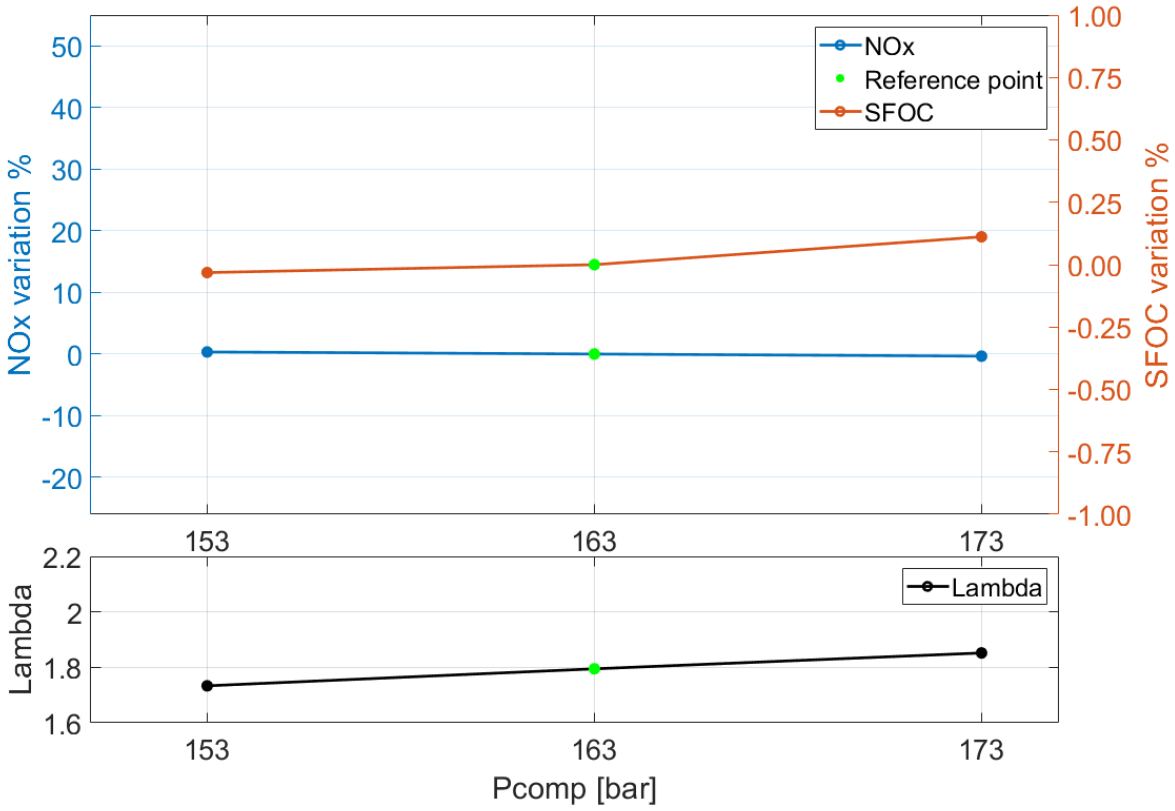

Figure 26: Compression pressure, Normalized SFOC NOx and lambda

$\mathbf{P_{comp}}$ **[bar]**	**Trapped air [-]**	**Fuel [-]**	**AF [-]**
153	0.965	0.999	24.8
163	1	1	25.7
173	1.03	1.001	26.5

Table 15: Air-fuel data at different compression pressures

6 Results: Dual fuel : Control on

In this section, the results of the engine running on Dual Fuel (Diesel pilot injection and Methane main injection) with all PID control systems active (IMEP control, Pmax control, Pcomp control, and maximum injection pressure control) are presented.

6.1 Nozzle diameter and Number of nozzle holes variation

As already explained in the diesel case (Section 4.1), reducing the diameter of the nozzle of the gas injector increases the injection duration, slows down the combustion, and requires advancing the SOI of the Methane, while the pilot injection remains constant for all the sweeps. These effects are shown in Figure 27, where the nozzle diameter is varied from 2.5 mm to 4.5 mm

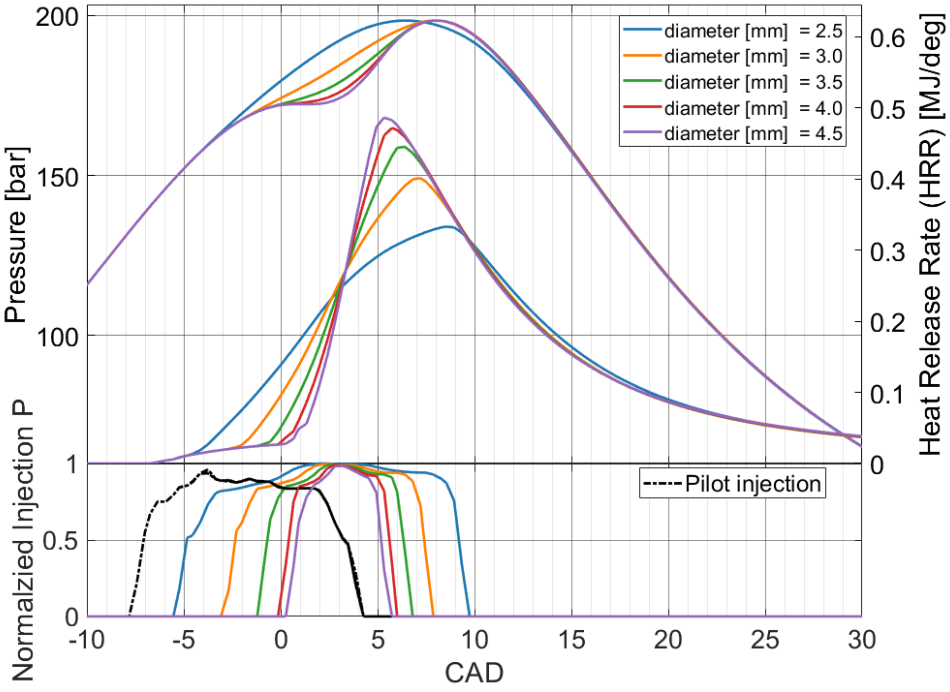

Figure 27: Hole diameter (Methane) variation, HRR P vs CAD

Looking at Figure 28, it can be seen that a similar behavior to the nozzle diameter variation case is also observed when the number of holes is changed.

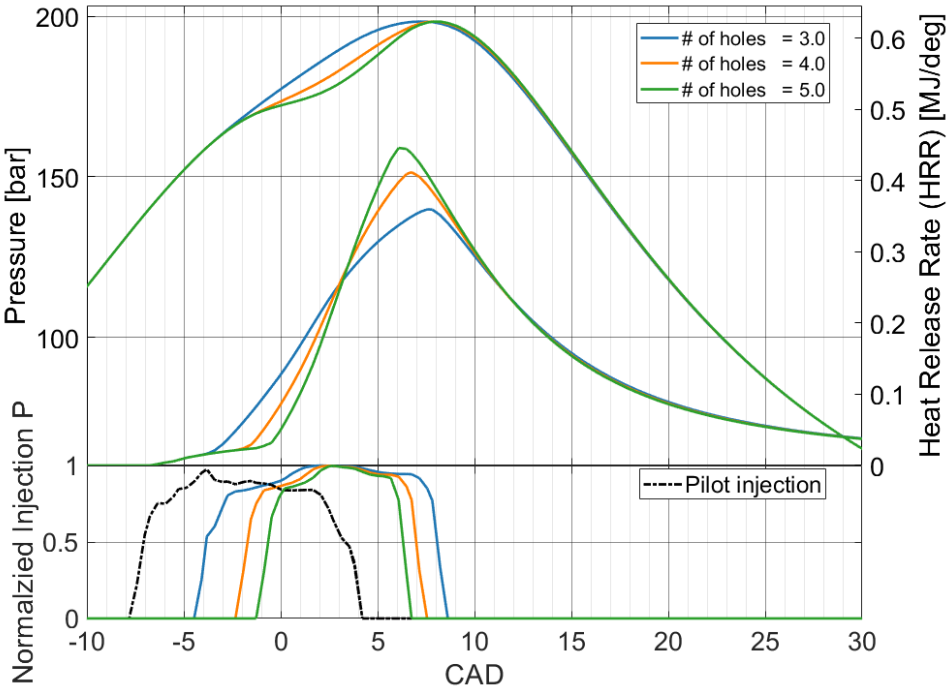

Figure 28: Number of holes (Methane) variation, HRR P vs CAD

Figure 29 shows that a reduction in nozzle diameter from 3.5 mm to 3.0 mm results in an SFOC improvement of approximately 0.05%, along with a reduction in NOx emissions of 10%. The trends are similar to those observed in the diesel engine; thus, also in this case, the change in SFOC between reducing the flow area by changing the hole diameter or the number of holes can be related to their influence on air entrainment.

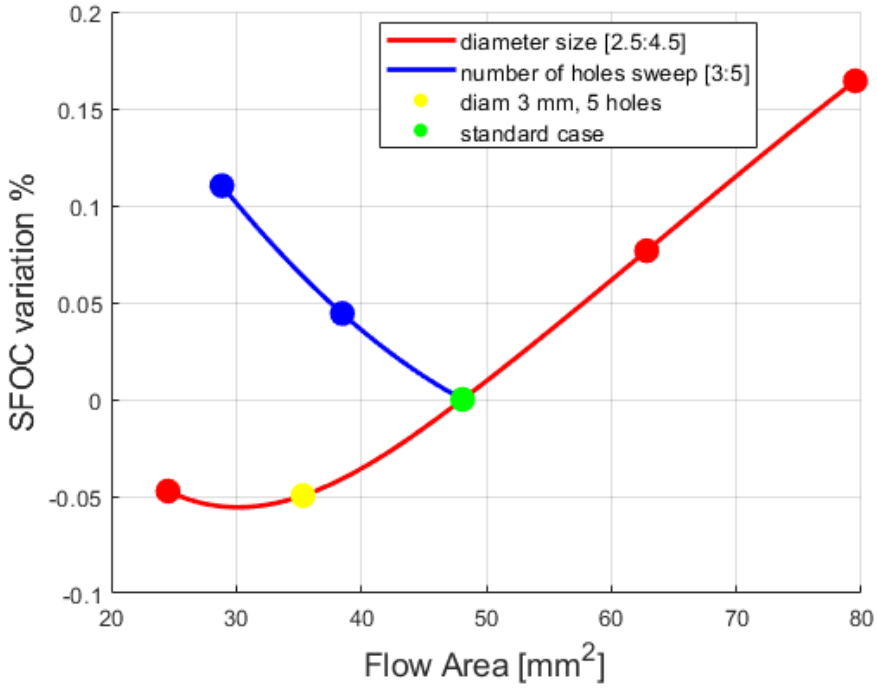

Figure 29: Flow area variation, Normalized SFOC, NOx

6.2 EGR level variation

The EGR level is varied from 0% to 23.8%. The heat release rate exhibits the expected trend, as shown in Figure 30. With lower EGR levels, the peak HRR is higher and the gas SOI is retarded to meet the target maximum pressure, while the pilot injection is kept fixed.

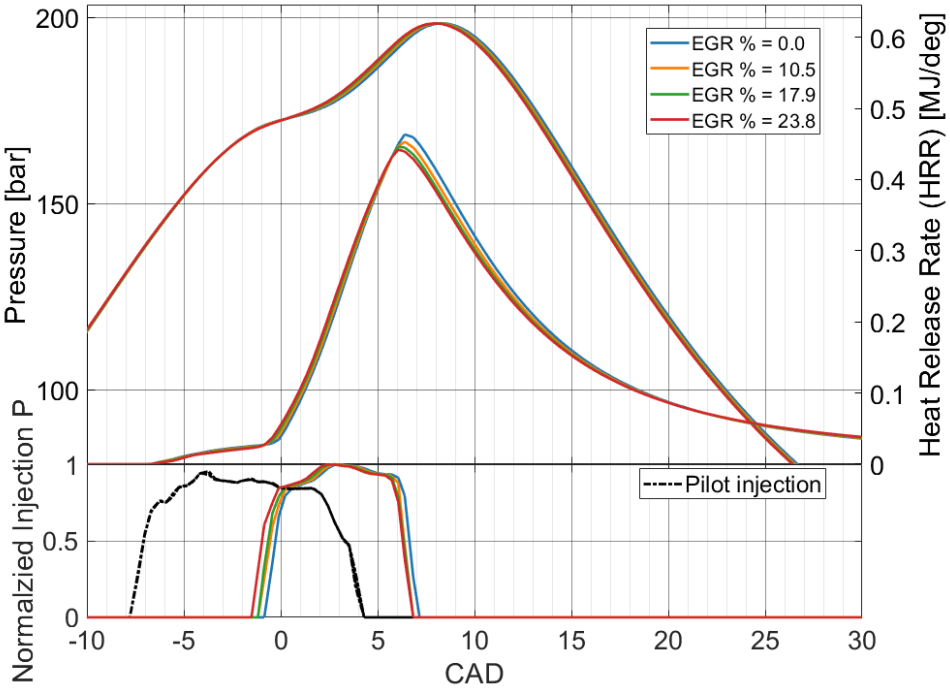

Figure 30: EGR level variation, HRR P vs CAD

From Figure 31, the trends for NOx, λ, and SFOC are evident. As expected, increasing the EGR level reduces λ due to less fresh air entering the cylinder. NOx emissions decrease with higher EGR, as also expected. However, SFOC reaches a minimum value at 10.5% EGR. At 0% EGR, SFOC is slightly higher, likely due to greater heat losses as shown in Table 16, which occur because higher temperatures are reached and also because the SOI is delayed, leading to a slightly retarded HRR peak.

Therefore, at 10.5% EGR, an SFOC reduction of approximately 0.51% is achieved, while NOx emissions increase by 18.46%.

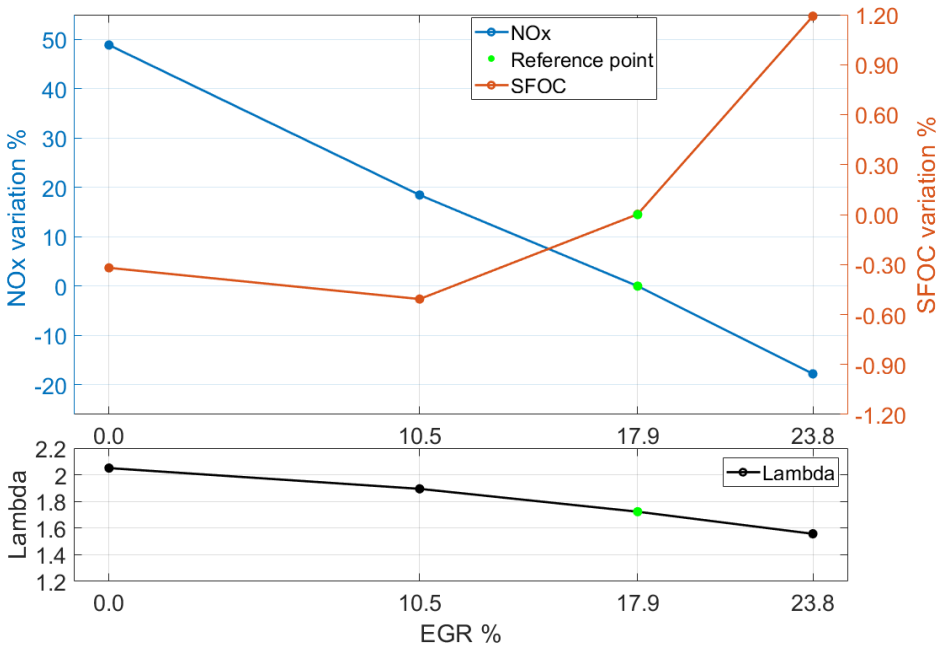

Figure 31: EGR level variation, Normalized SFOC, NOx

EGR %	0	10.5	17.9	28.8
Cumulative Heat Losses [MJ]	31.5	30.3	30.4	31.1

Table 16: Cumulative heat losses at different EGR percentages.

6.3 Geometric compression ratio variation

The geometric compression ratio has been varied by changing the shim thickness. From Figure 32, a trend in the heat release rate (HRR) can be observed: a higher geometric compression ratio leads to faster combustion, this is an unexpected trend because all the controllers are active , meaning that both the maximum cylinder and maximum motoring pressure are kept constant. In order to maintain a fixed compression pressure (P_{comp}), increasing the geometric compression ratio results in a delayed exhaust valve closing (EVC) time, which leads to less trapped air in the cylinder.

As a consequence, lambda decreases. Due to the reduced oxygen availability, a slower combustion process would be expected.

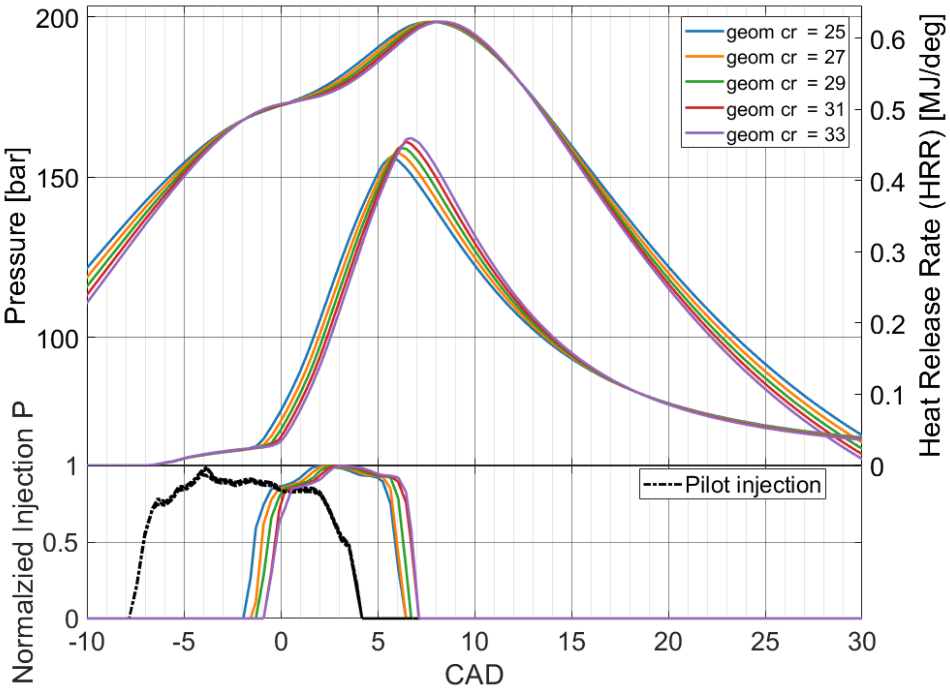

Figure 32: Geometric compression ratio variation, HRR P vs CAD

Table 17: Injection duration as a function of the geometrical compression ratio

Geometrical compression ratio [-]	25	27	29	31	33
Injection duration [CAD]	7.38	7.35	7.28	7.26	7.25

From Figure 33 it can be observed that SFOC and NOx exhibit opposite trends with respect to the geometric compression ratio. Specifically, SFOC decreases as the compression ratio increases, while NOx increases. This behavior is consistent with the HRR trend shown in Figure 32. SFOC reaches its minimum at a geometric compression ratio of 33, after which it slightly rises up to a CR of 39, mainly due to the delayed combustion. At CR = 33, a reduction in SFOC of 0.39% is achieved, accompanied by an increase in NOx emissions of 9.7%.

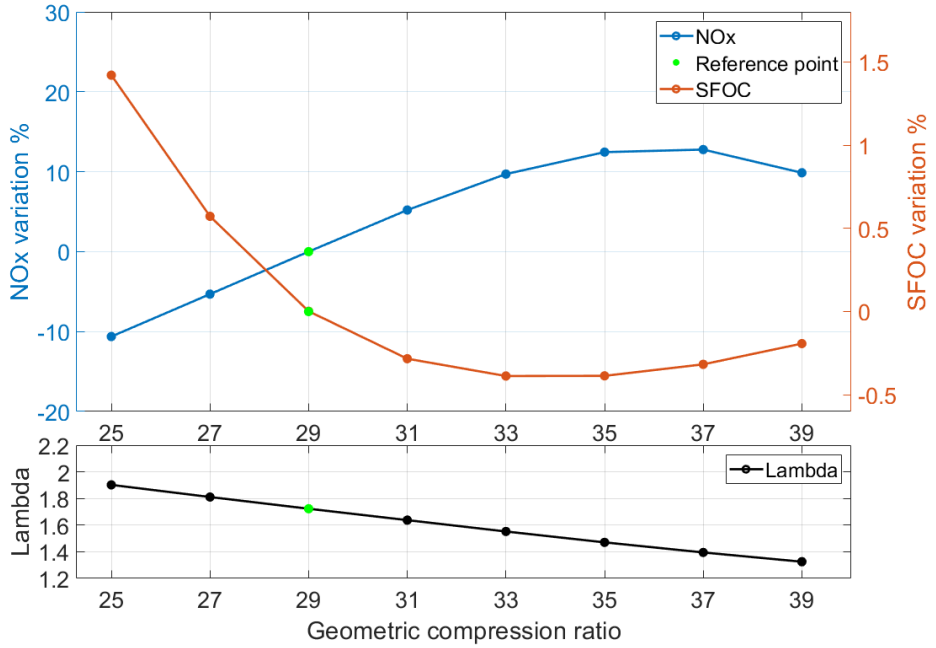

Figure 33: Geometric compression ratio variation, Normalized SFOC, NOx

6.4 Pilot on/off

Figure 34 shows the heat release rate (HRR) and pressure profiles for two cases: one in which the engine operates with a diesel pilot injection combined with a main methane injection (the standard dual-fuel case), and one in which only methane is injected (i.e., the pilot injection is removed). It can be observed that even without the diesel pilot, methane is able to ignite. This is because, at the SOI, the temperature inside the combustion chamber is already above the auto-ignition temperature of methane. Moreover, due to the absence of the pilot injection, the methane injection timing is slightly advanced, resulting in a higher HRR peak.

In Figure 35, it can be seen that at the start of injection (SOI), the in-cylinder temperature is higher than the auto-ignition temperature of methane. Specifically, at SOI $= -1.619$ CAD, the cylinder temperature is 766.9 °C, which is above the Methane auto-ignition temperature of 640 °C for Lambda of 1.71 [10].

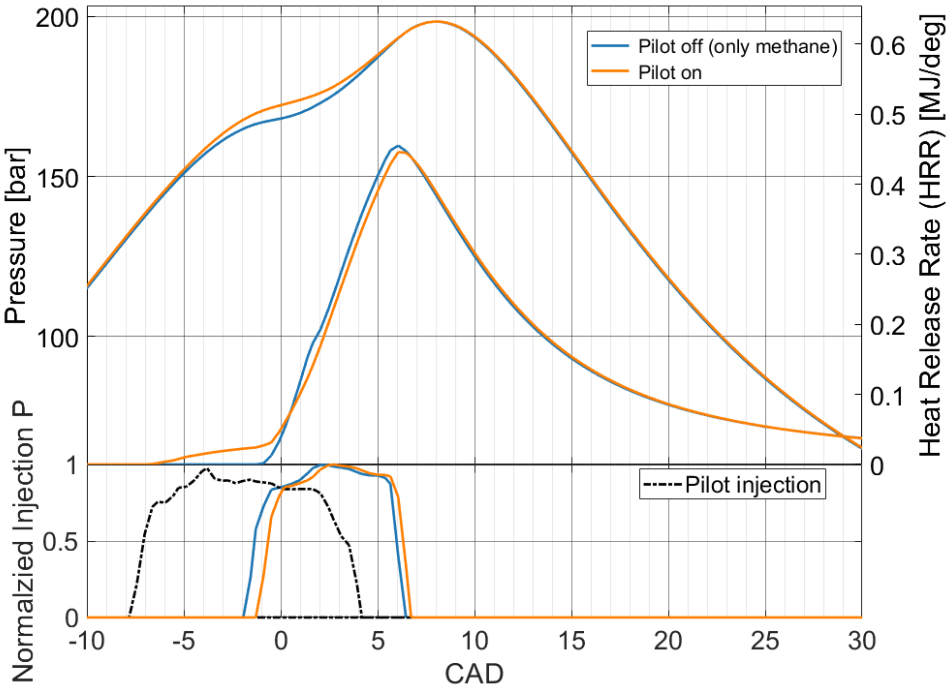

Figure 34: Pilot on/off, HRR P vs CAD

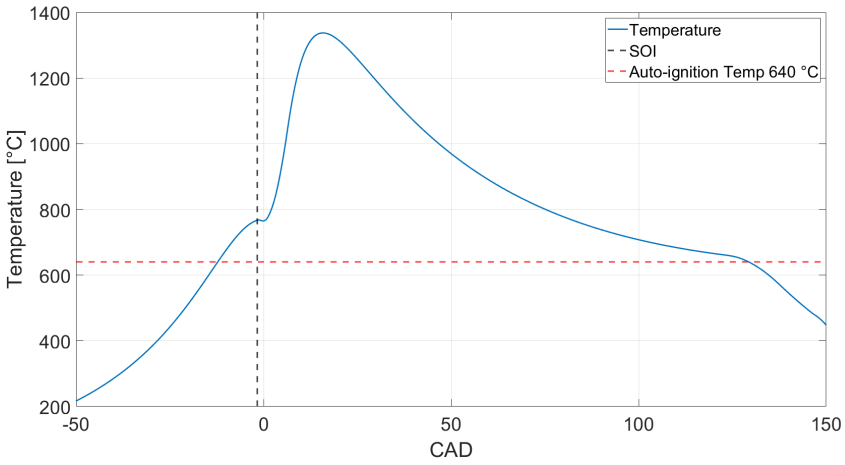

Figure 35: Pilot on/off, Temperature vs CAD

The absence of the pilot injection allows for lower fuel consumption; however, it results in a slightly lower indicated efficiency due to the difference in heating values, as shown in Table 18. NOx emissions increase with the pilot injection. This is because the presence of the pilot injection does not sufficiently slow down the combustion and it increases the in-cylinder pressure near top dead center (TDC), leading to higher combustion temperatures and, consequently, higher NOx emissions. So, without the pilot injection, there was a reduction in SFOC and NOx emissions of 0.33% and 7.71%, respectively. However, this result is not entirely reliable, as the model was calibrated using diesel pilot injection. Although the pilot amount is very small and the results without it are likely still valid, we cannot be 100% certain about this outcome.

Table 18: Comparison of engine performance parameters with and without pilot injection

Parameter	**Pilot off**	**Pilot on**
Normalized SFOC [-]	0.997	1
Normalized IE [-]	0.994	1
Normalized NOx [-]	0.92	1

6.5 Pilot injection duration variation

The pilot injection duration is varied while keeping the end of injection at a fixed CAD. In order to change the pilot injection duration without affecting the maximum injection pressure, the nozzle configuration is modified by adjusting the number and size of the holes.

As shown in Figure 36, no significant changes in the heat release rate (HRR) are observed; the HRR peak remains nearly constant. The only noticeable difference is related to the different start of injection (SOI). A longer pilot injection duration results in an earlier SOI, leading to a slightly more advanced pressure rise near top dead center (TDC). Although this may benefit thermal efficiency, the impact is negligible, as the pilot fuel quantity is very small and does not significantly influence engine performance.

As shown in Figure 37, both NO_x emissions and SFOC remain nearly constant. Slight performance deterioration is observed when the injection duration is reduced. Additionally, the values are influenced by the differences in the injector's geometric parameters, since both the number and diameter of the holes were modified to keep the maximum injection pressure constant, as detailed in Table 19.

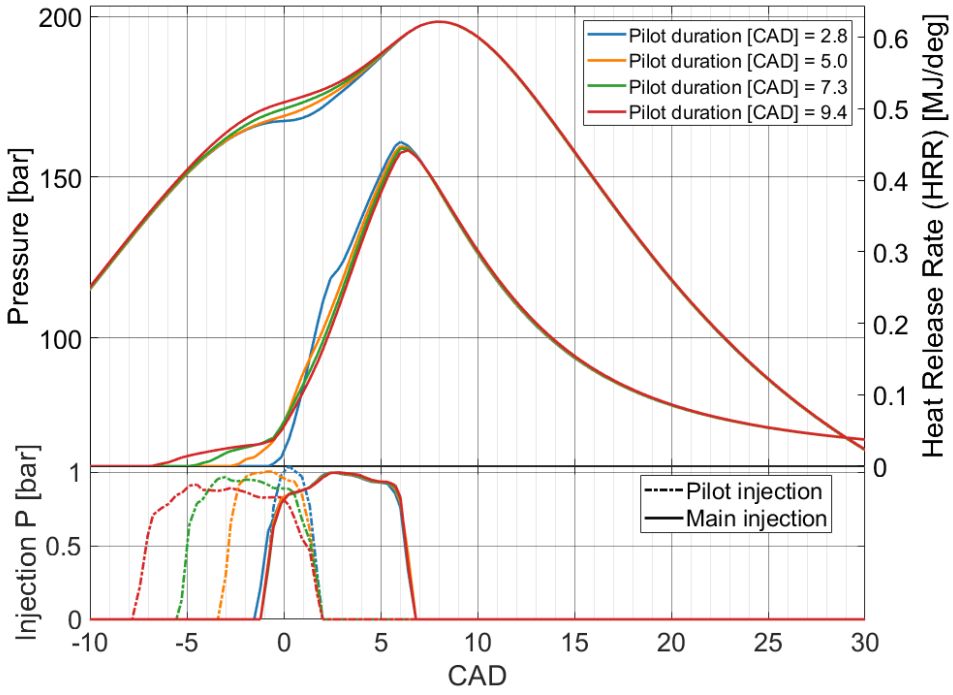

Figure 36: Pilot injection duration variation vs CAD

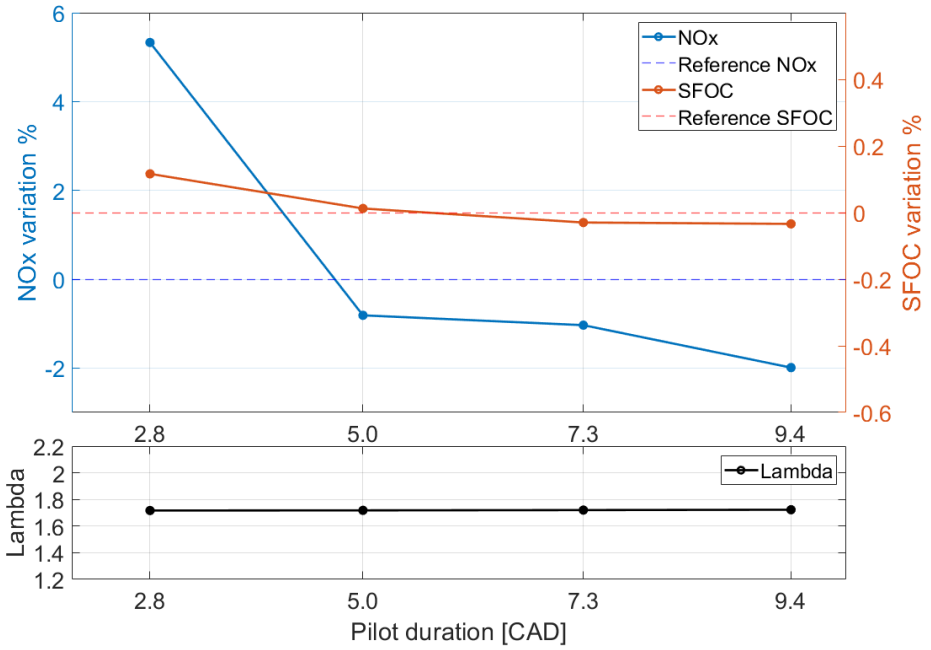

Figure 37: Pilot injection duration variation, Normalized SFOC, NOx

Table 19: Injector parameters varition (Standard conditions: 3 holes, diameter 0.55 mm, injection duration 11.26 CAD

Injection duration [CAD]	2.8	5	7.3	9.4
Hole diameter [mm]	0.95	0.67	0.55	0.48
Number of holes [-]	5	5	5	5

6.6 Pilot Start of injection variation

Figure 38 shows that variations in the start of injection (SOI) do not significantly affect the heat release rate (HRR). It can be observed that retarding the SOI leads to a slight increase in the HRR peak. This also results in a small reduction in fuel consumption and a slight increase in NOx emissions, as shown in Figure 39. Overall, by delaying the SOI pilot from -7.5 to -5.5 a reduction in SFOC of 0.04% and an increase in NOx 0.64% of can be achieved These are very small changes.

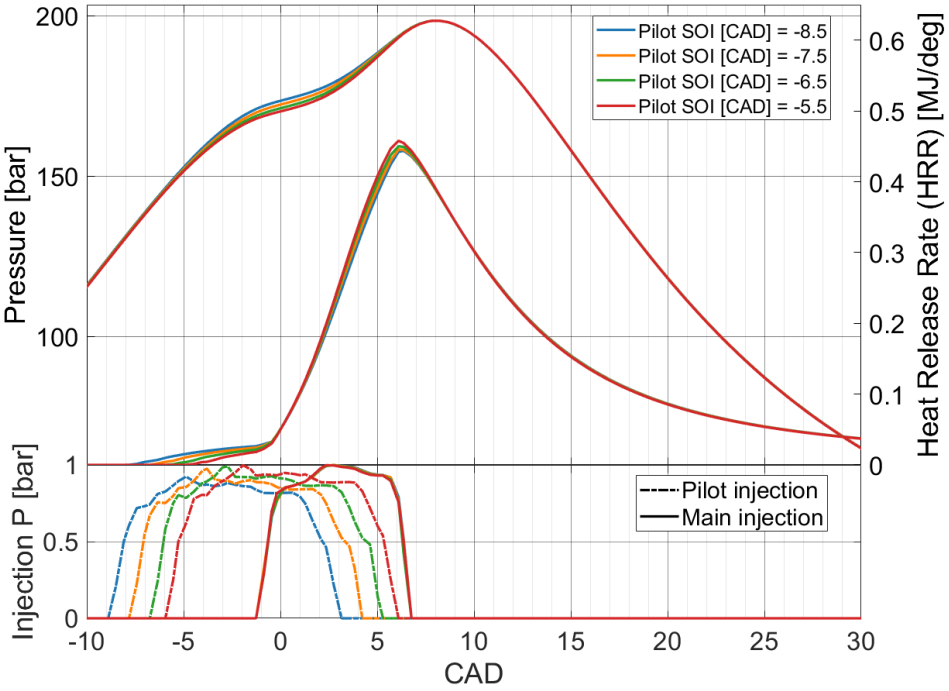

Figure 38: Pilot SOI variation vs CAD

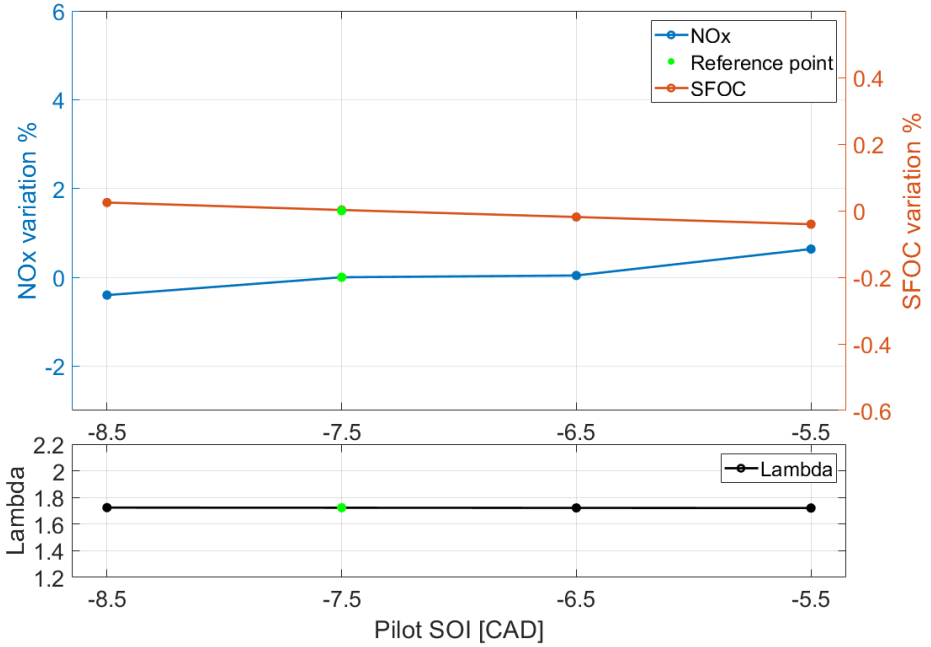

Figure 39: Pilot SOI variation, Normalized SFOC, NOx

6.7 Pilot fuel amount variation

The amount of pilot fuel injected is increased from the initial value of 6.5% of the main injection up to 33.8% (decreasing the amount of pilot in a large engine would lead to instability problems). As shown in Figure 40, increasing the pilot mass leads to a lower HRR peak, resulting in a slower combustion process. At the same time, the pressure near top dead center (TDC) increases due to the greater amount of heat released from the pilot injection.

As a result, Figure 41 shows that both fuel consumption and NO_x emissions increase. Interestingly, NO_x emissions rise even though increasing the pilot mass leads to slower combustion. This suggests that NO_x formation is more strongly influenced by the combustion of diesel fuel. It would be interesting to perform a simulation in which only the diesel pilot is injected, in order to evaluate how much NO_x would be emitted. However, this is not feasible, because at such low load conditions, the energy available would be insufficient to drive the turbine, and the compressors would therefore not be adequately supplied. Lambda remains almost constant; it is slightly decreasing. This is because the amount of trapped air is almost constant (the EVC time has not changed significantly). Despite more pilot fuel being injected, the amount of methane injected is reduced. As can be seen in Table 21, the total amount of fuel injected increases, with a maximum value of 1.9%. Therefore, the air-fuel ratio, and thus lambda, are not significantly affected.

Also in this case, in order to maintain a constant maximum injection pressure for the pilot, the diesel injector geometry was modified, as reported in Table 20.

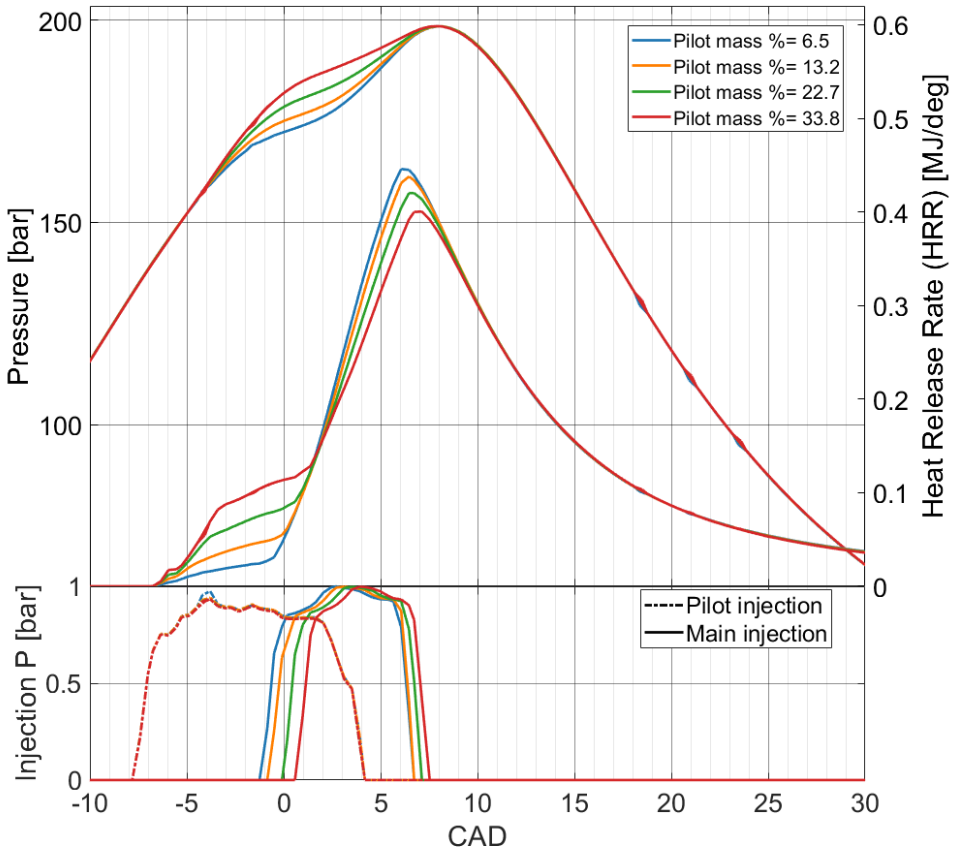

Figure 40: Pilot mass variation vs CAD

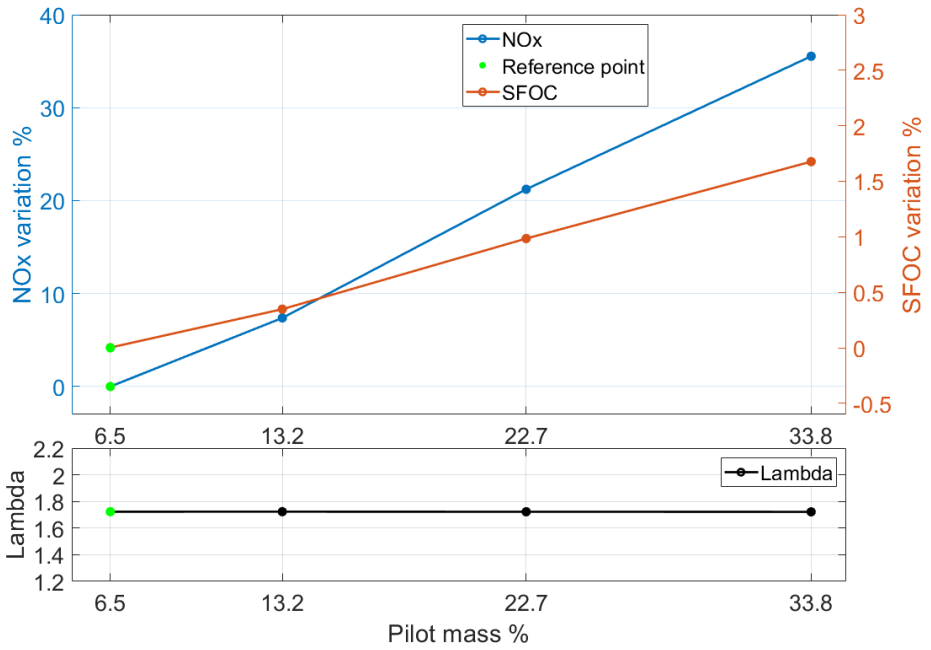

Figure 41: Pilot mass variation, Normalized SFOC, NOx

Table 20: Pilot injection parameters

Mass pilot %	6.5	13.2	22.7	33.8
Hole diameter [mm]	0.55	0.591	0.75	0.88
Number of holes [-]	3	5	5	5

Injected Pilot %	6.5	13.2	22.7	33.8
Total Injected Mass Variation %	0.00%	0.42%	1.15%	1.90%

Table 21: Variation of total injected mass with respect to the injected pilot %.

7 Results: Dual fuel control off

In this section, the results of the engine running on Dual Fuel (Diesel pilot injection and Methane main injection) with one or more PID control systems deactivated are presented.

7.1 Maximum cylinder pressure variation

In this case, the start of injection (SOI) of the gas is adjusted to achieve different peak pressures inside the cylinder. Advancing the gas injection allows more time for methane to mix with air, increasing both the heat release rate (HRR) peak and the in-cylinder pressure. With a SOI (gas) of -2.98 CAD, a maximum pressure of 218.5 bar is reached while Pcomp is kept fixed at 167.4 bar.

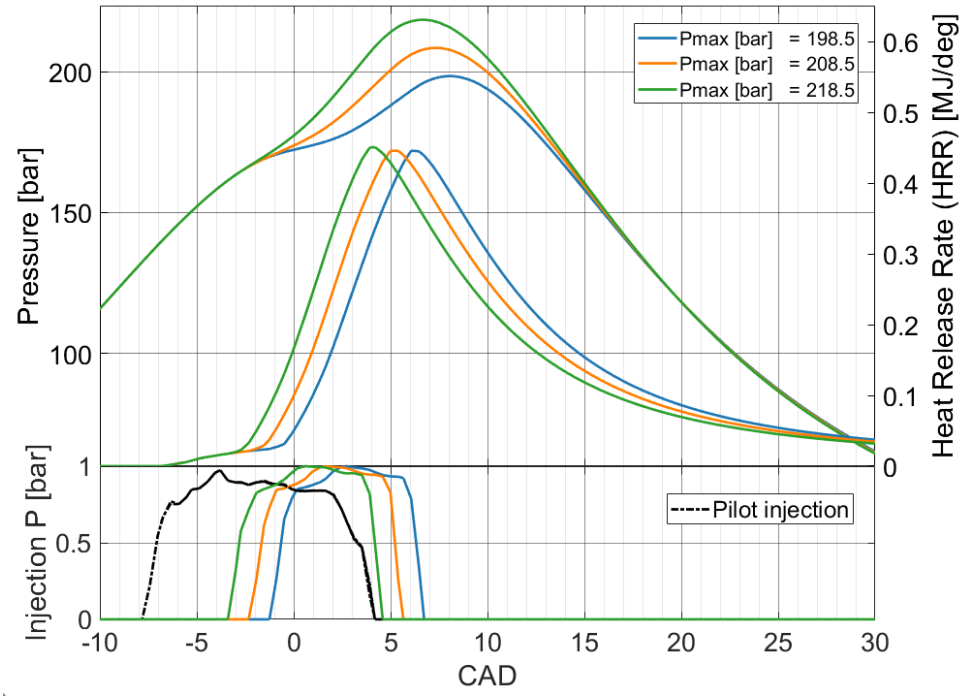

Figure 42: Maximum cylinder pressure variation vs CAD

As a result of the increased temperature, Figure 43 shows that with a maximum pressure of 218.5 bar, an increase in NOx emissions of 16.88%, along with a reduction in specific fuel oil consumption (SFOC) of 1.62%. The reduction in SFOC is related to the improvement in thermodynamic efficiency. In fact, by advancing the injection, the Methane has more time to mix with air, the HRR peak increases and shifts closer to top dead center (TDC), leading to a higher peak pressure and consequently a more effective expansion stroke.

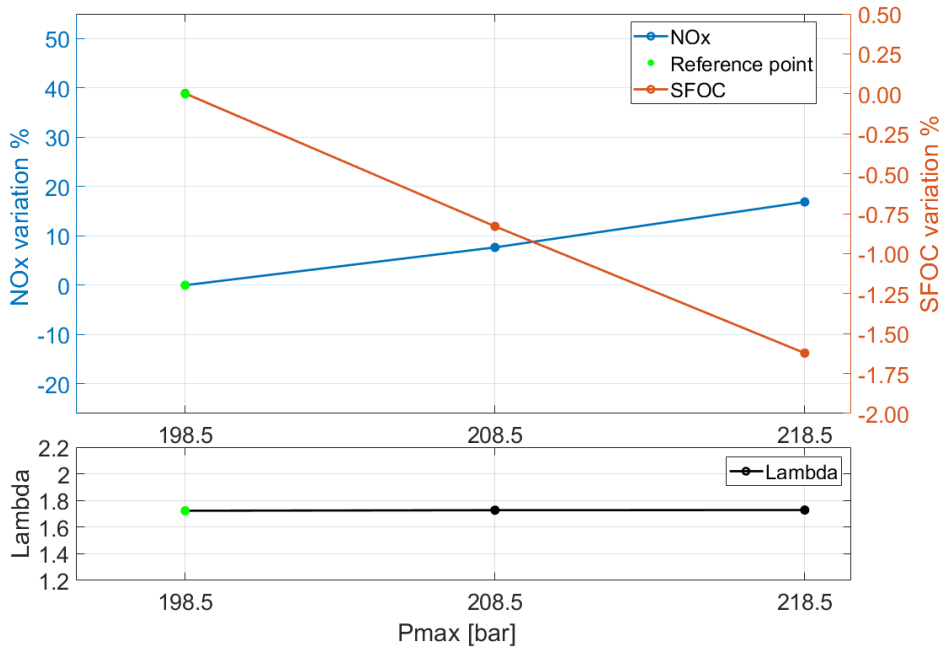

Figure 43: Maximum cylinder pressure variation, Normalized SFOC, NOx

7.2 Maximum cylinder pressure variation with a fix Pmax-Pcomp

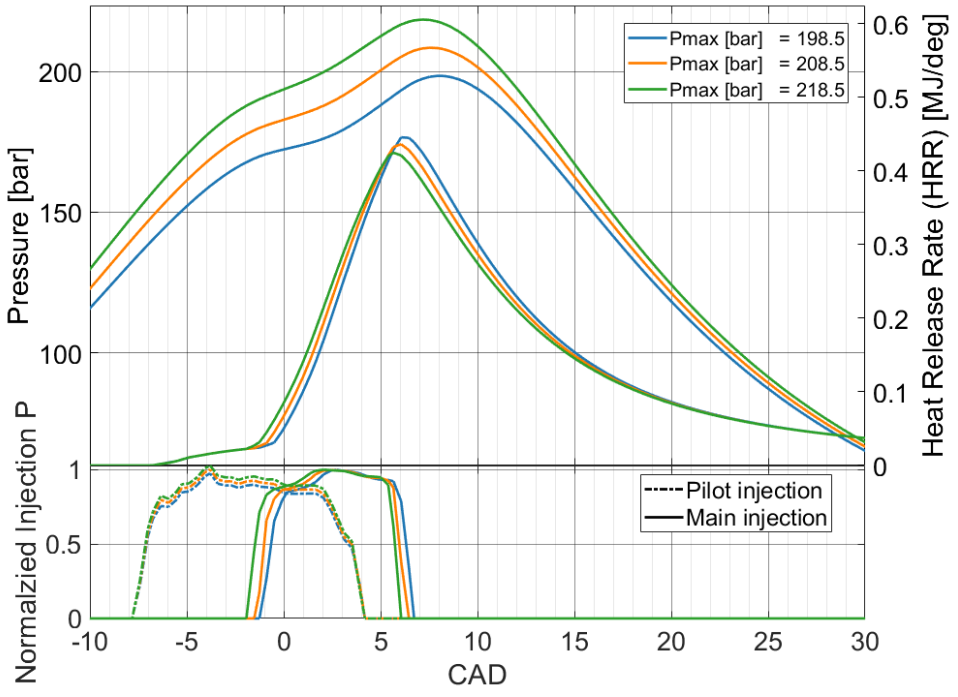

Figure 44: Maximum cylinder pressure variation with Pmax-Pcomp fixed vs CAD

$P_{\max}$ is varied together with the compression pressure (P_{comp}) in order to maintain a constant difference $P_{\max} - P_{\text{comp}}$ across all cases. Increasing $P_{\max}$ allows for an advanced start of injection (SOI) of the gas—in this case at -1.81 CAD—but at the same time, P_{comp} also increases due to an earlier exhaust valve closing (EVC), which results in more trapped air and thus a higher lambda (λ).

Despite this, a lower heat release rate (HRR) peak is observed. This is because when P_{comp} changes, the cylinder pressure during injection changes as well, leading to a longer injection duration that slows down combustion, the same as found for pure diesel case.

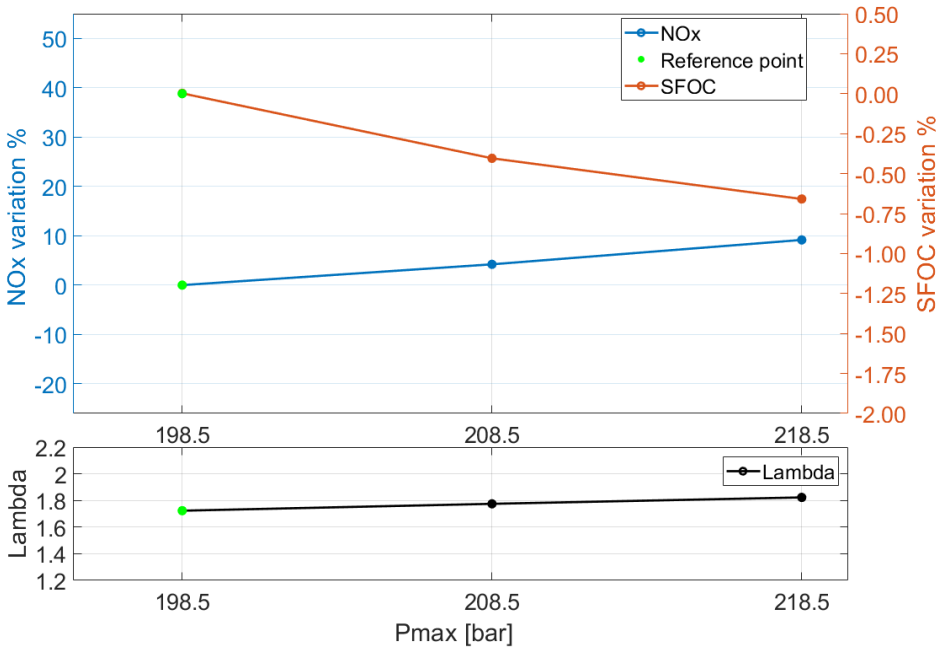

Figure 45: Maximum cylinder pressure variation with fixed $P_{\text{max}} - P_{\text{comp}}$: Normalized SFOC and NOx.

Although higher in-cylinder pressures are still achieved and the HRR peak remains advanced, as showed in Fig 45, this condition allows for improved efficiency, leading to a reduction in specific fuel oil consumption (SFOC) of 0.66% and an increase in NO_x emissions of 9.16%.

7.3 Compression pressure variation

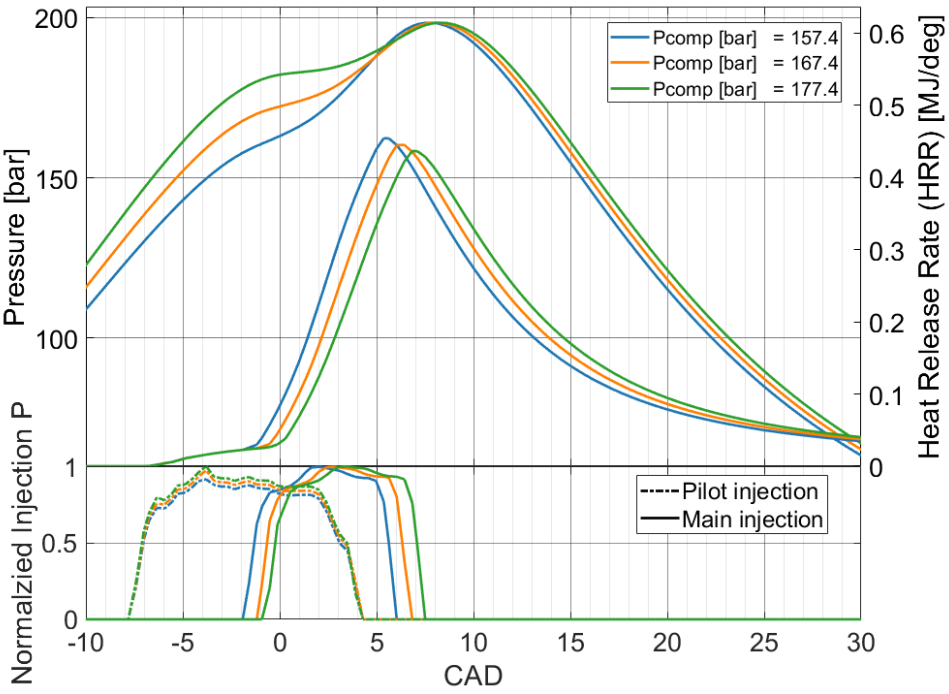

Figure 46: Compression pressure variation vs CAD

The compression pressure is controlled by the exhaust valve closing (EVC) timing, as shown in Figure 46. Reducing the compression pressure allows methane to be injected earlier due to the lower in-cylinder temperature at the start of injection (SOI). The advancement of the SOI shifts the heat release rate (HRR) peak closer to top dead center (TDC), improving thermal efficiency.

However, it can be noted that the HRR peak is lower at higher compression pressures. This occurs because a higher P_{comp} results in a longer injection duration, which slows down the combustion process.

As shown in Figure 47, by reducing the compression pressure by 10 bar (from 167.4 to 157.4 bar), a reduction in specific fuel oil consumption (SFOC) of 0.31% is achieved. However, this comes at the cost of a 5.17% increase in NO_x emissions due to the higher temperatures reached for the steeper HRR. Additionally, λ increases with higher P_{comp} because advancing the EVC timing increases the trapped air mass in the cylinder, thereby increasing the air–fuel ratio.

.

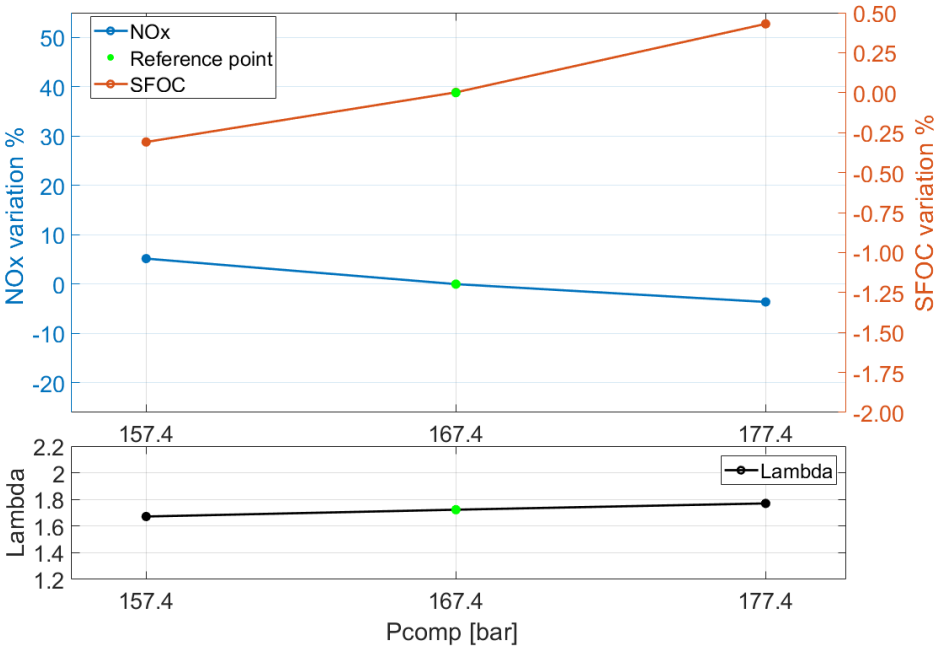

Figure 47: Compression pressure variation, Normalized SFOC, NOx

.

7.4 Maximum Injection Pressure Variation

In this case, the constraint on the maximum injection pressure for gas injection is removed. As shown in Figure 48, the injection duration is reduced to investigate the effect, while the pilot injection remains fixed. It can be observed that increasing the maximum injection pressure leads to a delay in the start of injection (SOI) of methane. This occurs because higher injection pressure improves atomization and mixing of the fuel with air [11], resulting in faster combustion. In fact, an increase in the heat release rate (HRR) peak can also be observed with higher injection pressures.

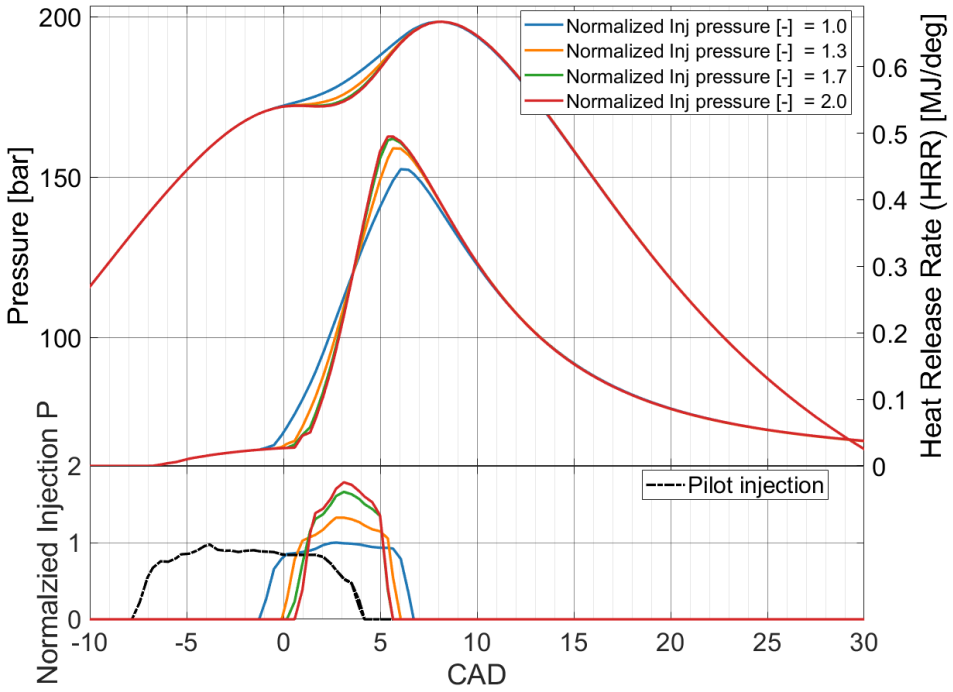

Figure 48: Maximum injection pressure variation (gas) vs CAD.

The effect of the delayed SOI can also be seen in the specific fuel oil consumption (SFOC) in Figure 49, which increases with higher injection pressure. Additionally, NO_x emissions rise due to the higher HRR peak achieved.

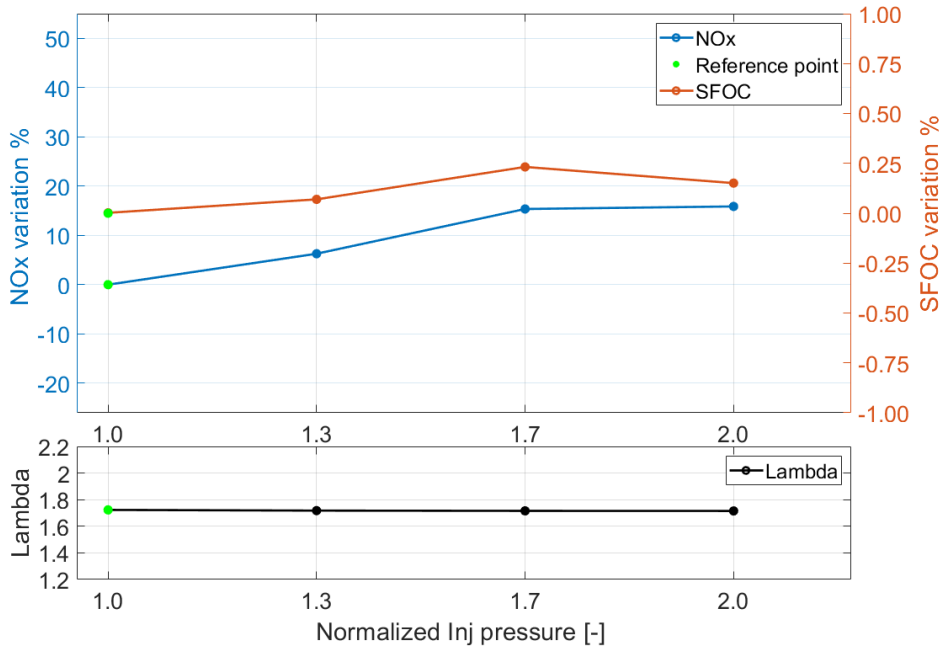

Figure 49: Effect of maximum injection pressure variation on SFOC and NO_x.

8 Discussion

In this study, the engine performance results of the G95 engine operating either in diesel-only mode or in dual-fuel mode (diesel pilot with methane main injection) are compared. The parameters varied in most cases are the same for both configurations. The main difference lies in the presence of the pilot injection in the dual-fuel mode, which allows additional focus on pilot-specific parameters such as the amount of fuel injected, pilot duration, and Start of injection — parameters considered only in the dual-fuel case.

Figure 50 displays the standard reference cases for both configurations.

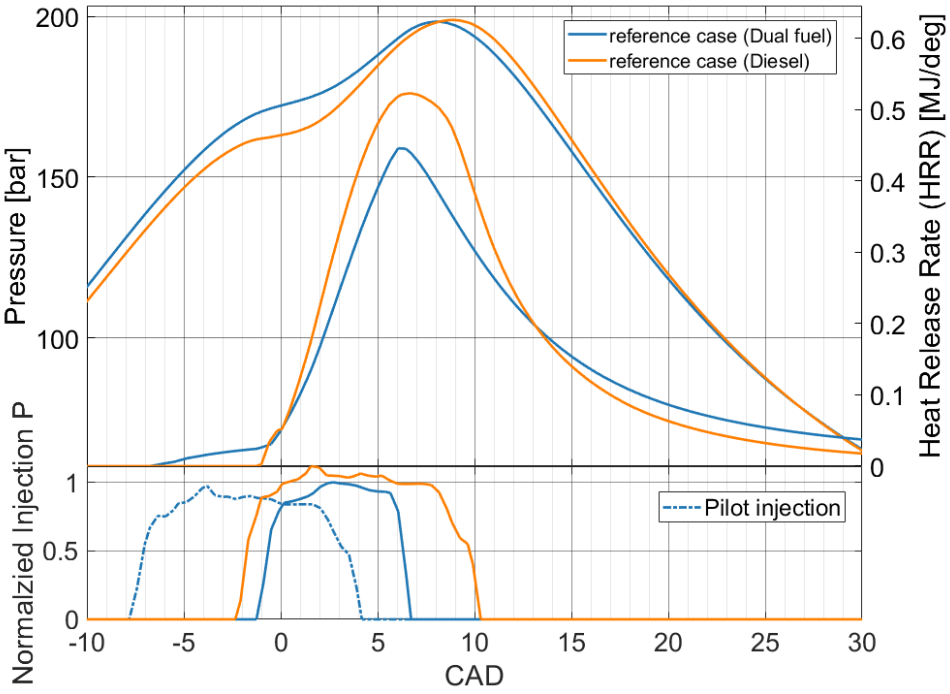

Figure 50: Comparison between diesel-only and dual-fuel (diesel-methane) operation.

These two baseline optimizations can be considered sufficiently tuned, given the many constraints applied. Despite this, it can be observed that the diesel-only engine provides higher indicated efficiency and SFOC than the dual-fuel one, this is mainly related to the way Indicated efficiency and SFOC are defined and the different heating values LHV of diesel and methane. However, the slower combustion process with methane injection contributes to lower NOx emissions.

An important observation from the results is that it is difficult to achieve significant improvements in engine performance when all the controllers are active. This is because the available degrees of freedom are limited; as a result, any change in a single parameter is counteracted by the controllers' responses to maintain constraints, leading to only marginal variations in efficiency.

From the results summarized in Figure 51, the relationship between SFOC and NOx emissions is plotted for both the diesel engine and the dual-fuel configuration. Each chart can be conceptually divided into four quadrants, with quadrants 1, 2, and 3 being the most relevant.

In Quadrant 1 and 3, a clear trade-off between SFOC and NOx emissions is observed: reducing SFOC typically leads to an increase in NOx, and vice versa. Quadrant 2, however, represents the most desirable operating region—where both lower SFOC and reduced NOx can be achieved. Unfortunately, this area is difficult to reach.

For the diesel engine, a reduction in NOx without significant impact on SFOC (quadrant

2) can be achieved by increasing the geometric compression ratio. In contrast, in the dual-fuel engine, simultaneous reductions in NOx and SFOC can be obtained either by reducing the gas injector nozzle hole diameter or by eliminating the pilot injection.

In Quadrant 3, the lowest SFOC values are found, but these come at the cost of increased NOx emissions. This behavior occurs particularly when one or more constraints are relaxed, for example, by allowing higher maximum cylinder pressure ($p_{\max}$).

Overall, it is evident that achieving significant improvements while satisfying all constraints is quite challenging (represented by the blue dots). However, when some control constraints are relaxed especially $p_{\max}$ greater reductions in SFOC become achievable (represented by the red dots).

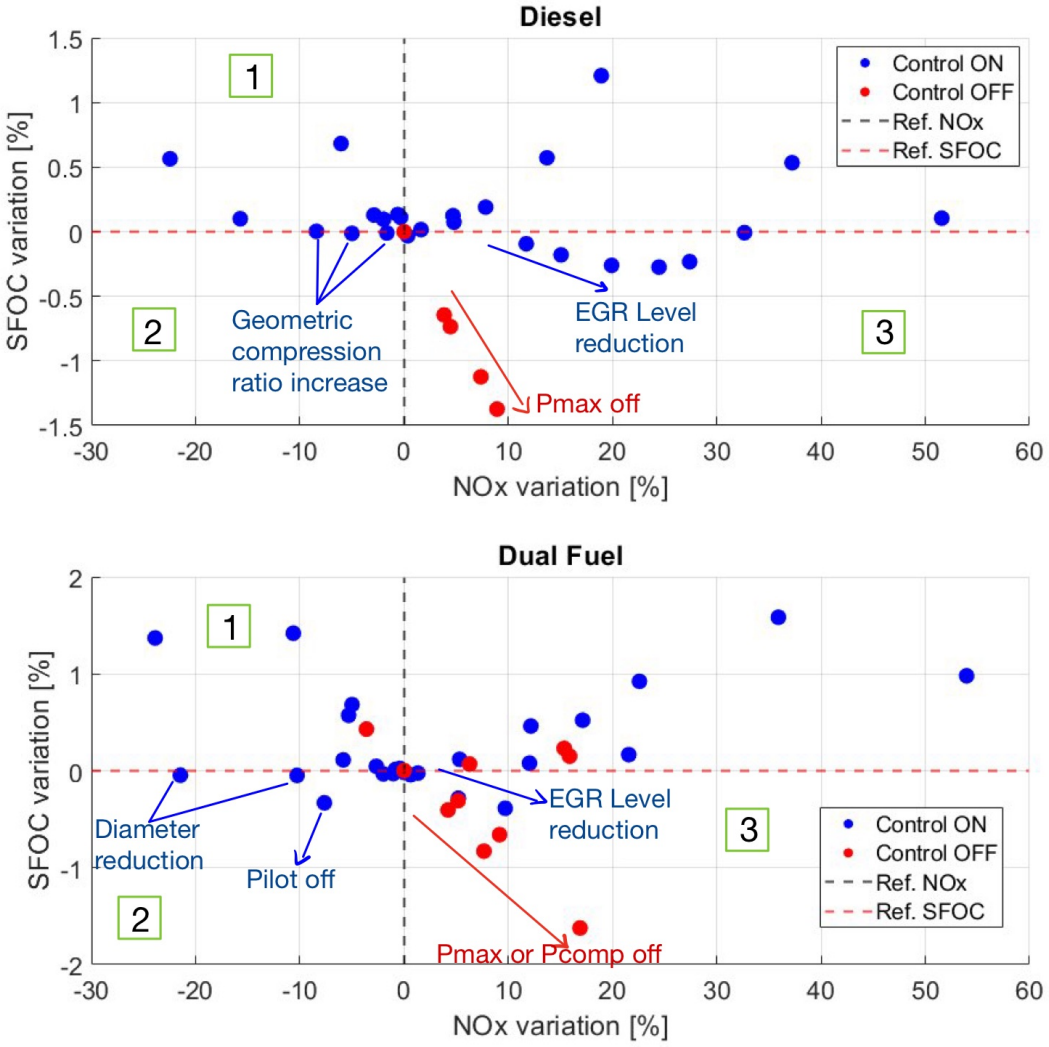

Figure 51: SFOC vs NOx .

Overall, similar trends are observed between the two configurations in terms of HRR shape, NO_x, and SFOC. The only notable difference between the two models lies in the HRR behavior during the geometric compression ratio variation that affects NOx emissions. In fact, while in the diesel model no clear trend can be seen in the HRR peak and the combustion get slower by increasing the geometric compression ratio due to a lower Lambda, in the Dual Fuel model a clear trend in the HRR peak and a reduction in combustion duration is observed. Thus the different trend in combustion duration influence the NOx emissions 52.

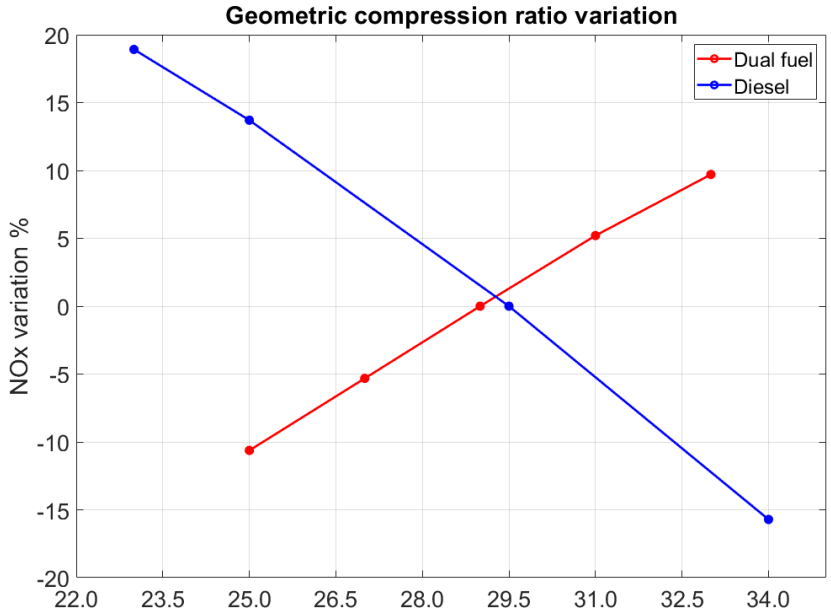

Figure 52: NOx emission Diesel vs Dual fuel (geoemtric compression ratio variation) %.

This occurs because the two models behave differently. While in the diesel model the reduction in Lambda with higher geometric compression ratio seems the reason behind the slower combustion, in the Dual Fuel instead despite the reduction in Lambda the combustion get faster,this is an unexpected behaviour that requires further investigation.

About the Dual Fuel engine, from the results, it can be observed that varying the pilot parameters does not have a significant effect. This is because the amount of pilot fuel is very small and does not substantially influence engine performance. However, by increasing the pilot mass injected, the impact on performance becomes more noticeable. It is also observed that the presence of the diesel pilot increases both fuel consumption and efficiency 53.

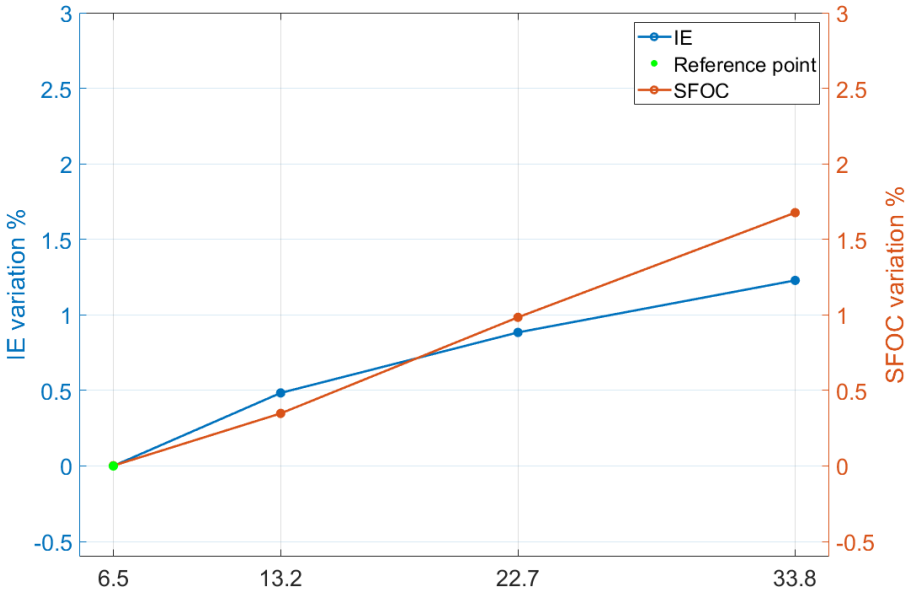

Figure 53: SFOC and Indicated efficiency VS mass pilot %.

This phenomenon can be explained by considering the different Lower Heating Values (LHV) of methane and diesel respectively 50 MJ and 42.5 MJ, as well as the definitions of indicated efficiency and SFOC in the corresponding formulas.

$$\eta_{ind} = \frac{IP}{\dot{m}_{diesel} \cdot LHVdiesel + \dot{m}_{methane} \cdot LHVmethane} \tag{17}$$

$$SFOC = \frac{\dot{m}_{diesel} + \dot{m}_{methane}}{BP} \tag{18}$$

Where:

- η_{ind} is the indicated efficiency
- W_{ind} is the indicated work
- $\dot{m}_{diesel}$ is the fuel mass flow rate of diesel
- $\dot{m}_{methane}$ is the fuel mass flow rate of methane
- LHV is the lower heating value of the fuel
- $SFOC$ is the specific fuel oil consumption

9 Conclusion

This study demonstrates that the engine whether operating in diesel-only mode or in dual-fuel configuration is well optimized overall. Improving engine performance under multiple constraints remains highly challenging. More than the shape of the heat release rate (HRR), what most significantly affects engine performance is the start of injection (SOI) and the timing at which the HRR peak occurs

As shown in Figure. 54, a reduction of 1 mm in the diesel nozzle diameter leads to a slight decrease in SFOC of 0.05%. Lowering the EGR level from 18.7% to 11.5% reduces SFOC by 0.27%, but also causes a significant increase in NOx emissions of 24.45%. Increasing the geometric compression ratio from 29.5 to 31 results in a 5% reduction in NOx without affecting SFOC. Further increasing the compression ratio to 31 while reducing EGR to 11.5% yields a 0.15% reduction in SFOC, accompanied by a 15% increase in NOx.

When fewer constraints are imposed, more substantial improvements can be achieved. For example, increasing the maximum cylinder pressure (Pmax) from 199 bar to 219 bar, while maintaining a constant pressure difference (Pmax - Pcomp = 36 bar), leads to a 1.12% reduction in SFOC and a 7.36% increase in NOx. Further increasing Pmax to 219 bar while keeping Pcomp fixed at 163 bar results in an SFOC reduction of 1.37% and a NOx increase of 8.92%.

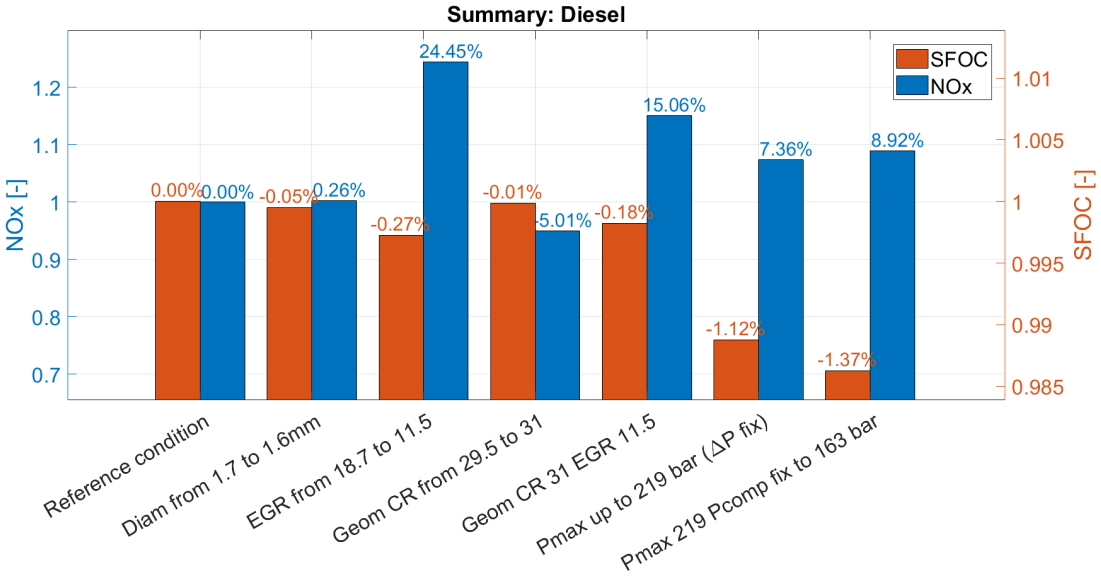

Figure 54: Summary: Diesel results

For the dual-fuel case, similar trends are observed. As shown in Figure. 55, reducing the methane nozzle diameter from 3.5 mm to 3 mm yields a slight SFOC decrease of 0.05%. Lowering EGR from 17.8% to 10.5% reduces SFOC by 0.51%, but increases NOx by 18.46%. Increasing the geometric compression ratio from 29 to 33 leads to a 0.39% reduction in SFOC and a 9.69% increase in NOx. Removing the diesel pilot results in a reduction of both SFOC and NOx by 0.33% and 7.65%, respectively.

Again, greater flexibility allows for more improvement. Increasing Pmax from 198.5 bar to 218.5 bar, while keeping the Pmax–Pcomp difference constant, results in a 0.66% reduction in SFOC and a 9.16% increase in NOx. Reducing Pcomp by 10 bar (from 167 bar to 157 bar) results in a 0.31% SFOC reduction and a 5.17% increase in NOx. Finally, increasing Pmax to 218.5 bar while keeping Pcomp fixed at 167 bar yields the best performance, with an SFOC reduction of 1.62% and a NOx increase of 16.88%.

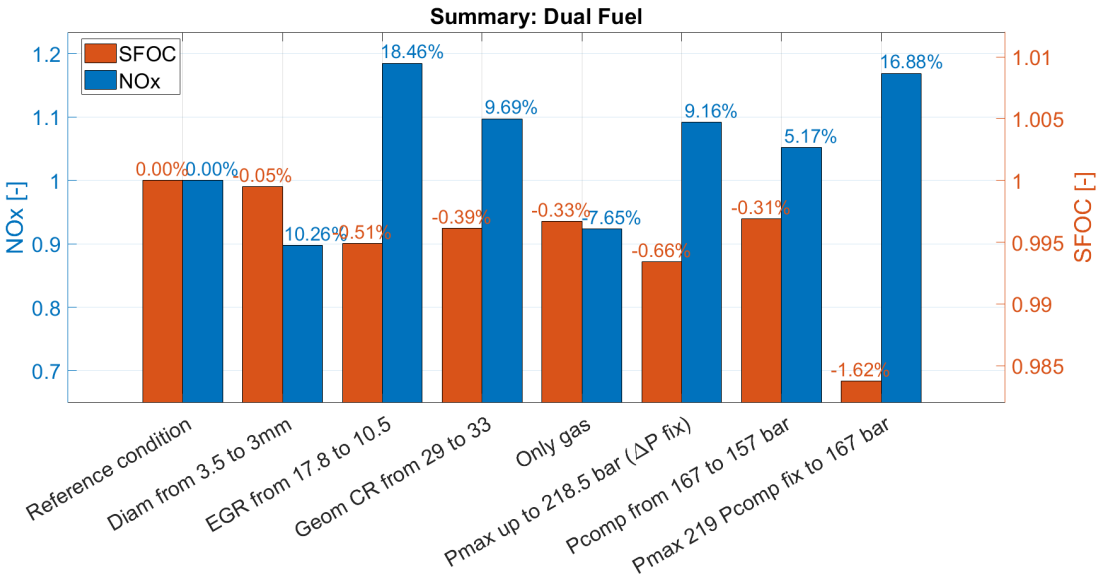

Figure 55: Summary: Dual-fuel results

In conclusion, for both diesel and dual-fuel configurations, increasing the maximum achievable pressure and the pressure difference between Pmax and Pcomp proves to be the most effective strategy for improving SFOC, while keeping NOx emissions within acceptable limits. This indicates that, in order to improve engine performance, varying the Start of Injection (SOI) and consequently shifting the combustion phasing has a strong impact, while modifying the heat release rate (HRR) shape has a minor effect.

References

[1] C. o. t. E. U. European Parliament, "Regulation (eu) 2021/1119 of the european parliament and of the council of 30 june 2021 establishing the framework for achieving climate neutrality and amending regulations (ec) no 401/2009 and (eu) 2018/1999 ('european climate law')," 2021.

[2] E. Commission, J. R. Centre, M. Crippa, D. Guizzardi, F. Pagani, M. Banja, M. Muntean, E. Schaaf, F. Monforti-Ferrario, W. E. Becker, R. Quadrelli, A. Risquez Martin, P. Taghavi-Moharamli, J. Köykkä, G. Grassi, S. Rossi, J. Melo, D. Oom, A. Branco, J. San-Miguel, G. Manca, E. Pisoni, E. Vignati, and F. Pekar, "Ghg emissions of all world countries," 2024.

[3] L. Gamma Technologies, "Gt power." Version used: GT-Power 2024.

[4] M. energy solutions, "Project guide g95me-c10.7," 2025.

[5] C. S. Godoy, "19 diesel engines," 2015.

[6] S. C. Sorenson, "Internal combustion engine principles," 2017.

[7] J. B. Heywood, "Internal combustion engine fundamentals," 1988.

[8] M. C. b. Cenk Sayin a, Metin Gumus a, "Influence of injector hole number on the performance and emissions of a di diesel engine fueled with biodieselediesel fuel blends," 2013.

[9] J. Ghojel, "Review of the development and applications of the wiebe function: A tribute to the contribution of ivan wiebe to engine research," 2010.

[10] C. ROBINSON and D. SMITH, "The auto-ignition temperature of methane," 1983.

[11] C. Yao, J. Hu, P. Geng, J. Shi, D. Zhang, and Y. Ju, "Effects of injection pressure on ignition and combustion characteristics of diesel in a premixed methanol/air mixture atmosphere in a constant volume combustion chamber," 2017.

List of Figures

List of Tables

10 Appendix

10.1 Diesel model validation

The values plotted represent the percentual variation between test data and simulated data, calculated using the following formula:

$$\text{Variation } (\%) = \left(\frac{\text{Test parameter}}{\text{Simulation parameter}} - 1 \right) \times 100$$

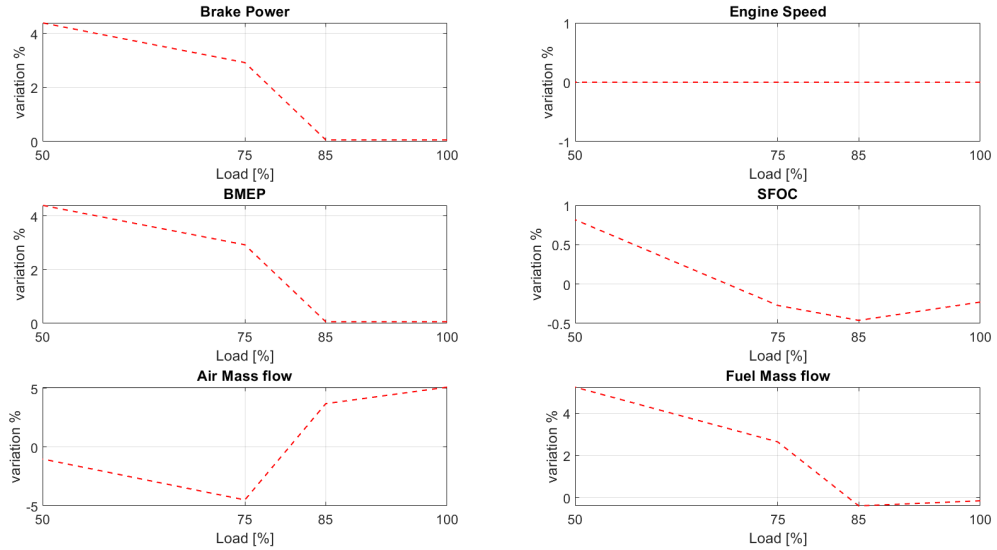

Figure 56: Variation for each load between test and simulation of : Brake Power, Engine speed, BMEP, SFOC, Air Mass flow, Fuel Mass flow, Diesel engine

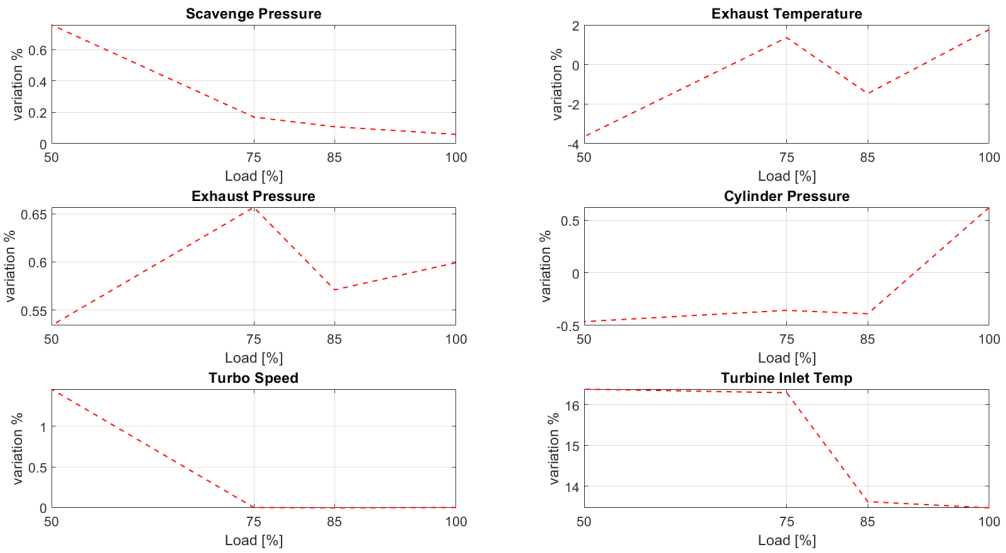

Figure 57: Variation for each load between test and simulation of : Scavenging pressure, Exhaust temperature, Exhaust pressure, Cylinder pressure, Turbo speed, Turbine inlet temperature, Diesel engine

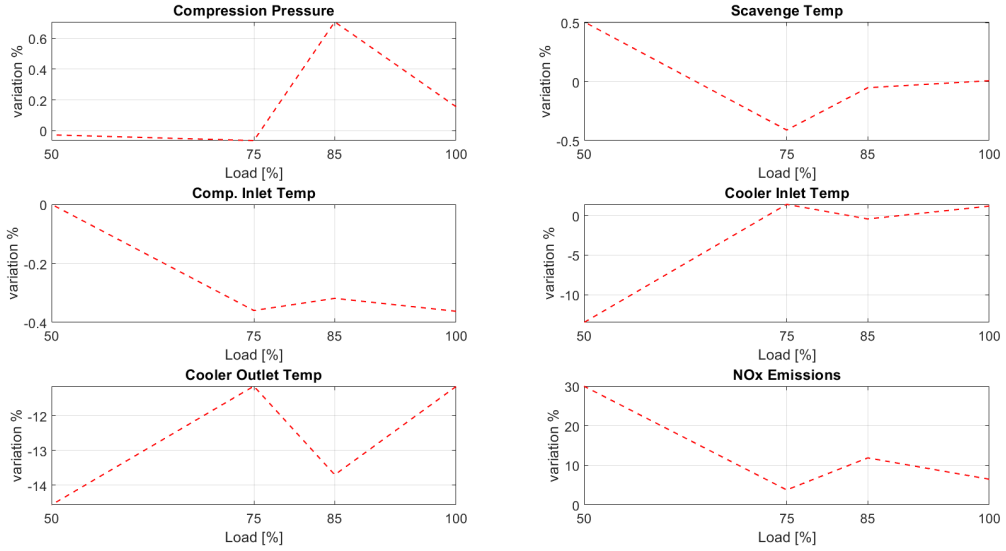

Figure 58: Variation for each load between test and simulation of : Compression pressure, Scavenging temperature, Compressor inlet temperature, Cooler inlet temperature, Cooler outlet temperature, NOx emissions, Diesel engine

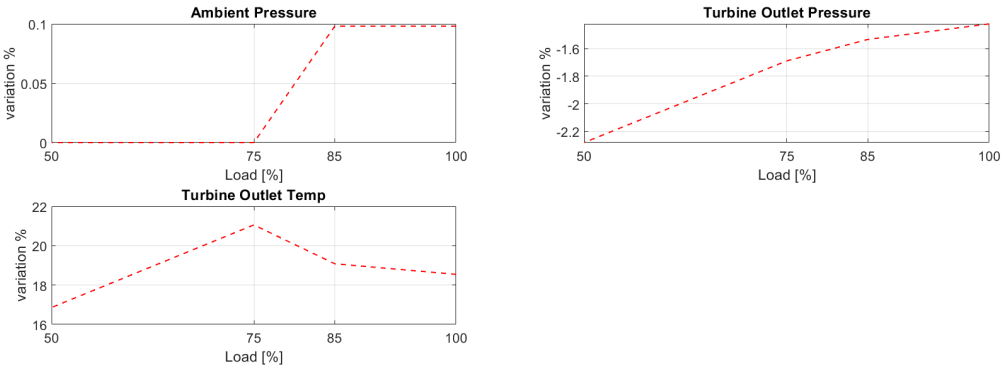

Figure 59: Variation for each load between test and simulation of : Ambient pressure, Turbine outlet pressure, Turbine outlet temperature, Diesel engine

10.2 Dual Fuel model validation

The values plotted represent the percentual variation between test data and simulated data, calculated using the following formula:

$$\text{Variation } (\%) = \left(\frac{\text{Test parameter}}{\text{Simulation parameter}} - 1 \right) \times 100$$

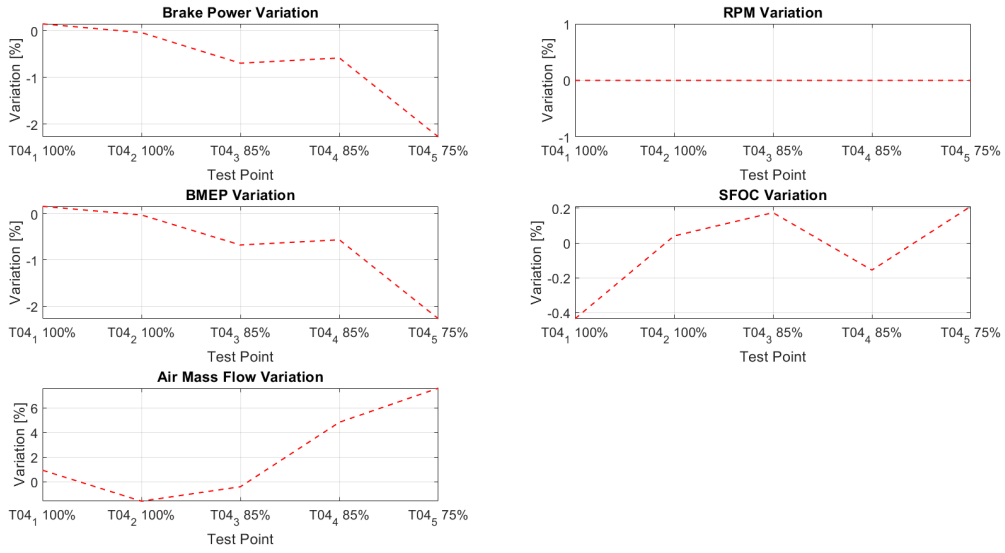

Figure 60: Variation for each load between test and simulation of : Brake Power, Engine speed, BMEP, SFOC, Air Mass flow, Fuel Mass flow, Dual Fuel engine

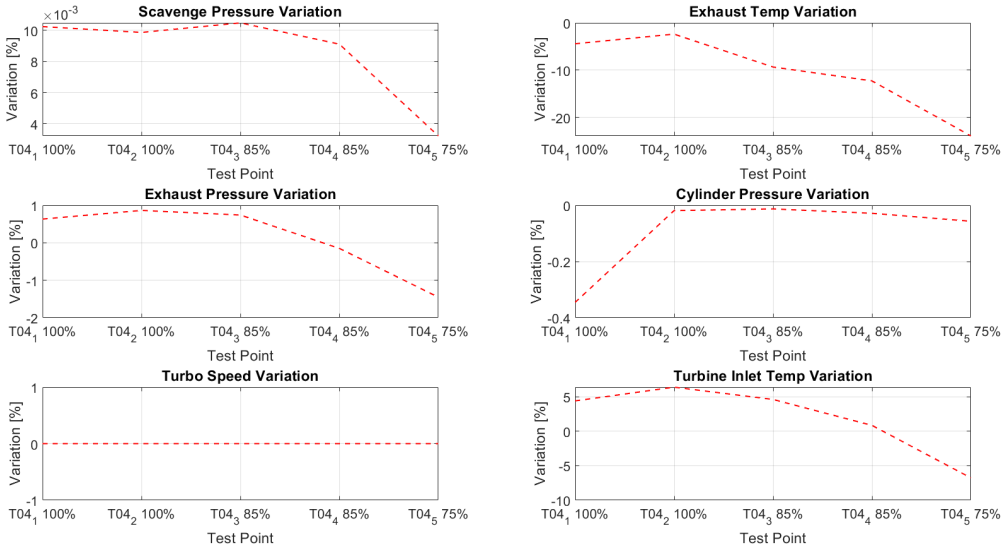

Figure 61: Variation for each load between test and simulation of : Scavenging pressure, Exhaust temperature, Exhaust pressure, Cylinder pressure, Turbo speed, Turbine inlet temperature,Dual Fuel engine

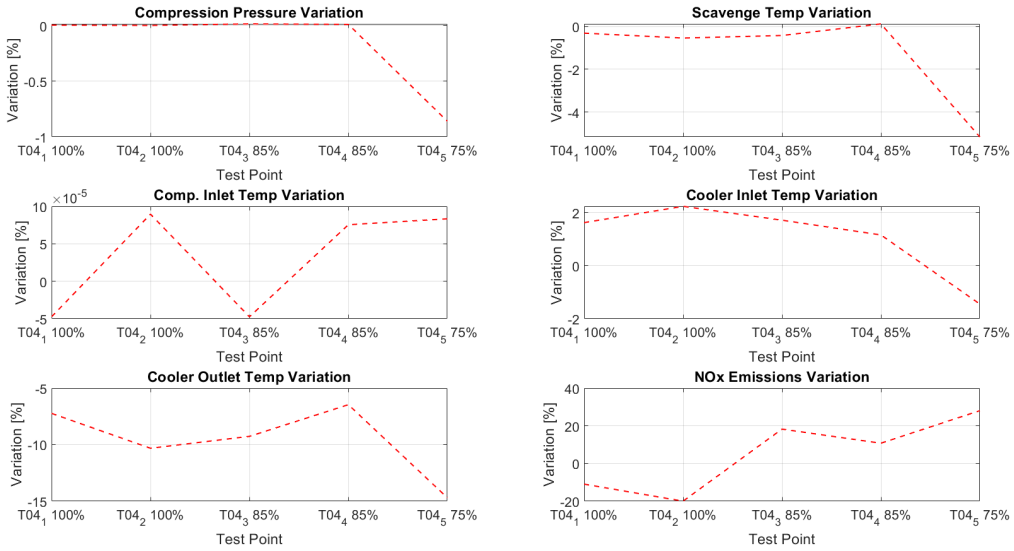

Figure 62: Variation for each load between test and simulation of : Compression pressure, Scavenging temperature, Compressor inlet temperature, Cooler inlet temperature, Cooler outlet temperature, NOx emissions, Dual Fuel engine

,

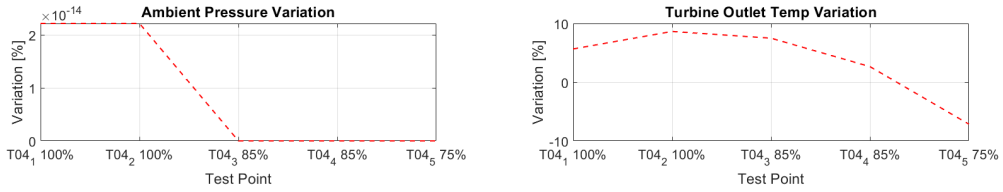

Figure 63: Variation for each load between test and simulation of : Ambient pressure, Turbine outlet pressure, Turbine outlet temperature, Dual Fuel engine

10.3 Matlab script for premixed energy calculation

```
1
2  %Heat release analysis
3  %%
4  %weibe function , EGR
5  clc
6  clear
7  close all;
8  %Input files
```

```
file1='C:\Users\ZMWORE\Desktop\Diesel_simulation\EGR\egr_control\egr_control_std.txt';
file2='C:\Users\ZMWORE\Desktop\Diesel_simulation\EGR\egr_control\egr_control_analysis.txt';
data1 = readmatrix(file1, "NumHeaderLines", 4);
data2 = readmatrix(file2, "NumHeaderLines", 3);

CAD = data1(:, 1);  %crank angle degree
HRR = data1(:, 2:5); % Heat release rate
SFOC=data2(:,5); %specific fuel oil consumption
CA50=data2(:,10)
width=data2(:,11)


%Wiebe fucntion
Wiebe = @(b, x) -b(1) * (1 - exp(-b(2) * ((x - b(3)) ./ b(4)).^b(5)))+b(1);
%0 EGR
A(1) = max(HRR(:,1));
    a(1) = 9.2;
    theta_start(1) =6.4 %6.9;
    duration(1) = width(1);
    m(1) =2.22 %2.19;
% 10.5 % egr
    A(2) = max(HRR(:,2));
    a(2) = 9.7%7.95;
    theta_start(2) =6.4 %6.9;
    duration(2) = width(2);
    m(2) =2.2 %2.19;
% 18.7% EGR
    A(3) = max(HRR(:,3));
    a(3) = 8.7%7.95;
    theta_start(3) =6.7 %6.9;
    duration(3) = width(3);
    m(3) =2.18 %2.19;
% 24% EGR
    A(4) = max(HRR(:,4));
    a(4) = 9.2;
    theta_start(4) =6.8 %6.9;
    duration(4) = width(4);
    m(4) =2.19 %2.19;     figure;

for i=1:4
    params(i,:) = [A(i), a(i), theta_start(i), duration(i), m(i)];
    a_v=[ 7.94 ]
    m_v=[ 2.19]
    colors = lines(length(a_v)); % Genera colori diversi
    HRR_Wiebe(:,i) = Wiebe(params(i,:), CAD);


%Plot
EGR_values = [0 11.5 18.72 24]; % Define EGR percentages


    subplot(2, 2, i);  % Create a 2x2 grid of subplots

    plot(CAD, HRR(:,i)./10^6, 'k-', 'LineWidth', 1.5, 'DisplayName', 'Simulated data'); % Simulated
    hold on;
    plot(CAD, HRR_Wiebe(:,i)./10^6, 'LineWidth', 2, 'DisplayName', 'Wiebe fit'); % Wiebe

    xlabel('Crank Angle Degree (CAD)');
    ylabel('Heat Release Rate [MJ/CAD]');
    xlim([-5 25]);
    grid on;
    legend('show');
    set(gca, 'FontSize', 20);
    title(sprintf('EGR %d%%', EGR_values(i)));
    hold off;
```

```
74
75      % Valid indices for premixed energy computation
76      valid_idx = HRR_Wiebe(:,i) > 0;
77
78      % Premixed energy calculation
79      Premixed_energy(i) = trapz(CAD(valid_idx), HRR_Wiebe(valid_idx, i))
80      tot_energy(i)=trapz(CAD, HRR(:,i));
81  end
82
83  %1plot
84  %%
85
86  Premixed_energy = real(Premixed_energy);
87  SFOC = real(SFOC);
88  %Premixed_energy=Premixed_energy./tot_energy
89
90  % Sorted values
91  [Premixed_sorted, idx] = sort(Premixed_energy);
92  SFOC_sorted = SFOC(idx);
93
94  % Interpolation
95  x_interp = linspace(min(Premixed_sorted), max(Premixed_sorted), 100);
96  y_interp = interp1(Premixed_sorted, SFOC_sorted/ref_SFOC, x_interp, 'linear');
97  figure
98  plot(x_interp, y_interp, 'b-', 'LineWidth', 2)
99  hold on
100 scatter(Premixed_energy, SFOC/ref_SFOC, 80, 'b', 'filled')
101 xlabel('Premixed energy [J]', 'FontSize', 20)
102 ylabel('Normalized SFOC [-]', 'FontSize', 20)
103 grid on
104 %legend('Scatter Data', 'Interpolated Line', 'FontSize', 20)
105 hold off
106
107
108 %%
109 %%
110 %weibe function , number of holes
111 clc
112 clear
113 clc; clear; close all;
114
115
116 file1='C:\Users\ZMWORE\Desktop\Diesel_simulation\number_of_holes\n_h_control\n_h_control_std.txt';
117 file2='C:\Users\ZMWORE\Desktop\Diesel_simulation\number_of_holes\n_h_control\n_h_control_analysis.
        txt';
118 data1 = readmatrix(file1, "NumHeaderLines", 4);
119 data2 = readmatrix(file2, "NumHeaderLines", 3);
120
121 CAD = data1(:, 1);
122 HRR = data1(:, 2:5);
123 SFOC=data2(:,5);
124 S_comb=data2(:,9)
125 CA50=data2(:,10)
126 width=data2(:,11)
127
128
129 %Wiebe fucntion
130 Wiebe = @(b, x) -b(1) * (1 - exp(-b(2) * ((x - b(3)) ./ b(4)).^b(5)))+b(1);
131 % 3 holes
132 A(1) = max(HRR(:,1))-5000;
133     a(1) = 20;
134     theta_start(1) =3.5 ;
135     duration(1) = width(1);
136     m(1) =2.15 ;
137 % 4  holes
```

```
    A(2) = max(HRR(:,2));
    a(2) = 13;
    theta_start(2) =5.3;
    duration(2) = width(2);
    m(2) =2.20 ;
% 5 holes
    A(3) = max(HRR(:,3));
    a(3) = 8.7;
    theta_start(3) =6.7 ;
    duration(3) = width(3);
    m(3) =2.18 ;

      hole_numbers = [3 4 5]; % Number of holes in each case
for i=1:3

    params(i,:) = [A(i), a(i), theta_start(i), duration(i), m(i)];
    a_v=[ 7.94 ]
    m_v=[ 2.19]
    colors = lines(length(a_v));
    HRR_Wiebe(:,i) = Wiebe(params(i,:), CAD);

    %PLOT
    subplot(2, 2, i);  % Subplot grid: 2 rows, 2 columns

    plot(CAD, HRR(:,i)./10^6, 'k-', 'LineWidth', 1.5, 'DisplayName', 'Simulated data');
    hold on;
    plot(CAD, HRR_Wiebe(:,i)./10^6, 'LineWidth', 2, 'DisplayName', 'Wiebe fit');

    xlabel('Crank Angle Degree (CAD)');
    ylabel('Heat Release Rate [MJ/CAD]');
    xlim([-5 25]);
    grid on;
    legend('show');
    set(gca, 'FontSize', 20);
    title(sprintf('Holes: %d', hole_numbers(i)));
    hold off;

    % Premixed energy calculation
    valid_idx = HRR_Wiebe(:,i) > 0;
    Premixed_energy(i) = trapz(CAD(valid_idx), HRR_Wiebe(valid_idx, i));
end

Premixed_energy = real(Premixed_energy);
SFOC = real(SFOC);

% Sorting data
[Premixed_sorted, idx] = sort(Premixed_energy);
SFOC_sorted = SFOC(idx);

% interpolation
x_interp = linspace(min(Premixed_sorted), max(Premixed_sorted), 100);
y_interp = interp1(Premixed_sorted, SFOC_sorted/ref_SFOC, x_interp, 'linear');

%Plot
figure
plot(x_interp, y_interp, 'b-', 'LineWidth', 2)
hold on
scatter(Premixed_energy, SFOC/ref_SFOC, 80, 'b', 'filled')
xlabel('Premixed energy [J]', 'FontSize', 20)
ylabel('Normalized SFOC [-]', 'FontSize', 20)
grid on
hold off
```